Received: 25 March 2022 | Revised: 17 May 2022 | Accepted: 17 May 2022

DOI: 10.1002/ar.25021

SPECIAL ISSUE ARTICLE

The Anatomical Record | WILEY

Rare juvenile material constrains estimation of skeletal allometry in *Gryposaurus notabilis* (Dinosauria: Hadrosauridae)

Jordan C. Mallon[1,2] | **David C. Evans**[3,4] | **Yuguang Zhang**[5] | **Hai Xing**[1,5,6]

[1]Beaty Centre for Species Discovery and Palaeobiology Section, Canadian Museum of Nature, Ottawa, Ontario, Canada

[2]Ottawa-Carleton Geoscience Centre and Department of Earth Sciences, Carleton University, Ottawa, Ontario, Canada

[3]Royal Ontario Museum, Toronto, Ontario, Canada

[4]Department of Ecology and Evolutionary Biology, University of Toronto, Toronto, Ontario, Canada

[5]Beijing Museum of Natural History, Beijing, People's Republic of China

[6]State Key Laboratory of Palaeobiology and Stratigraphy, Nanjing Institute of Geology and Palaeontology, CAS, Nanjing, People's Republic of China

Correspondence
Jordan C. Mallon, Beaty Centre for Species Discovery and Palaeobiology Section, Canadian Museum of Nature, Ottawa, ON K1P 6P4, Canada.
Email: jmallon@nature.ca

Funding information
Beijing Government; Beijing Millions of Talents Project in the New Century, Grant/Award Number: 2019A41; Canadian Museum of Nature; National Natural Science Foundation of China, Grant/Award Number: 41602006; Natural Science Foundation of Beijing Municipality, Grant/Award Number: 5174032; Natural Sciences and Engineering Research Council of Canada, Grant/Award Number: RGPIN-2018-06788; State Key Laboratory of Palaeobiology and Stratigraphy of the Nanjing Institute of Geology and Palaeontology, Grant/Award Number: 203120

Abstract

In studying the skeletal allometry of any vertebrate, it is important to sample the ontogenetic extremes to ensure the accuracy of parameter estimation; this is particularly true for fossil taxa, where sampling of ontogenetic series is incomplete and sporadic. Previous studies have examined allometry in the skull of the duck-billed dinosaur *Gryposaurus notabilis*, but these did not include individuals smaller than ~65% the maximum known size (based on linear dimensions). Here, we report on the two smallest known examples of this species (a mostly complete skeleton and a partial skull), which are ~37% the known maximal size of *G. notabilis*. Osteohistology indicates that these represent individuals ~2 years of age. Allometric analysis demonstrates that most aspects of the skull of *G. notabilis* grew isometrically, although the height of the nasal arch grew with positive allometry. Early in the ontogeny of *G. notabilis*, the dentary teeth possessed secondary ridges, which were lost later in life. This finding has important bearing on hadrosaurid tooth taxonomy. The limb proportions of *G. notabilis* largely grew isometrically (or with weak negative allometry, at most), like some other hadrosaurids, suggesting that the species did not undergo a gait shift with increasing age (unless it occurred very early in ontogeny). We argue that the lack of significant locomotory performance compensation exhibited by young hadrosaurids helps to explain why they apparently formed small, mutualistic aggregations, presumably for protection from large predators.

1 | INTRODUCTION

Hadrosauridae was a geographically widespread, large herbivorous dinosaur clade that was both diverse and highly abundant during the Late Cretaceous, particularly within western North America (Horner et al. 2004). As a function of this high abundance, hadrosaurids are ontogenetically well-sampled, informing our understanding of their ontogenetic niche ecology (Wyenberg-Henzler et al., 2022) and skeletal allometry (Evans, 2010; Wosik et al., 2017). Investigation of the latter topic has resulted in a flurry of recent publications on hadrosaurids, including *Hypacrosaurus altispinus* (Brink et al., 2011; Dodson, 1975; Evans, 2010), *Corythosaurus* spp. (Dodson, 1975; Evans, 2010), *Lambeosaurus* spp. (Dodson, 1975; Evans, 2010), and *Parasaurolophus* sp. (Farke et al., 2013) among lambeosaurines (hollow-crested hadrosaurids), and *Brachylophosaurus canadensis*, *Edmontosaurus annectens* (Prieto-Márquez, 2014a; Wosik et al., 2017), and *Saurolophus angustirostris* (Bell, 2011; Dewaele et al., 2015) among hadrosaurines (solid-crested and crestless hadrosaurids, Hadrosaurinae sensu Xing et al., 2017).

The subject of the present study concerns the hadrosaurid *Gryposaurus notabilis* Lambe 1913 from the Campanian Dinosaur Park Formation of Alberta (Ryan & Evans, 2005). Allometric growth in the skull of this species has garnered some attention, beginning with Waldman (1969) who was restricted to making largely qualitative observations, given the limited material available to him. More recently, Prieto-Márquez (2010) hypothesized that *G. "incurvimanus"* Parks 1919 was a junior synonym of *G. notabilis*, and that the traits typically used to diagnose the two species (mainly relating to the size and position of the characteristic nasal arch) are continuous between the two. In this way, he reasoned that the smaller *G. "incurvimanus"* represents a subadult growth form of *G. notabilis*, which retains taxonomic priority. Picking up on this work, Farke and Herrero (2014) further demonstrated that the dorsal cranial vault becomes more flexed in older *G. notabilis*. The most comprehensive analysis to date has been that of Lowi-Merri and Evans (2020), who applied linear and geometric morphometrics to demonstrate that both *G. "incurvimanus"* and *G. notabilis* fall on the same growth trajectory for all traits investigated. They further showed that these two morphs are not separated stratigraphically, as one might expect given the two-species hypothesis (Mallon, 2019). Lowi-Merri and Evans (2020) therefore supported the previous formal synonymization of these two species by Prieto-Márquez (2010).

A limitation of the work of Prieto-Márquez (2010) and Lowi-Merri and Evans (2020) is that they were unable to sample the smallest known individuals due to their incompleteness and other methodological limitations, constraining their ability to accurately estimate allometric growth parameters otherwise facilitated by sampling the end members of the growth trajectory. In this study, we describe the two smallest-known specimens that are positively attributable to *G. notabilis*: CMN 8784 and ROM 1939. These are approximately equal in size and are just ~37% the length of the largest known individuals. Neither specimen factored into the quantitative analyses of Prieto-Márquez (2010) or Lowi-Merri and Evans (2020), and have otherwise merited little mention in the literature. The exception is the skull of CMN 8784, which was described and illustrated by Waldman (1969). However, his comparisons were largely qualitative in nature and limited to the holotype skull of *G. notabilis* (CMN 2278). ROM 1939 has not yet been illustrated or described in the literature. We subject both skulls to linear allometric analysis to better constrain the cranial allometry of the species. CMN 8784 also includes a nearly complete, articulated postcranial skeleton, which Waldman did not figure, although he did briefly mention some peculiarities that set it apart from the holotype skeleton of *G. "incurvimanus"* (ROM 764). This small skeleton also affords an opportunity to examine allometric trends in the postcranium, and to compare to trends described for other hadrosaurids (e.g., Farke et al., 2013; Guenther, 2014; Wosik et al., 2017).

1.1 | Institutional abbreviations

AMNH, American Museum of Natural History, New York, New York, U.S.A.; CMN, Canadian Museum of Nature, Ottawa, Ontario, Canada; MSNM, Museo di Storia Naturale di Milano, Milano, Italy; ROM, Royal Ontario Museum, Toronto, Ontario, Canada; TMP, Royal Tyrrell Museum of Paleontology, Drumheller, Alberta, Canada.

1.2 | Anatomical abbreviations

art, articular; ast, astragalus; ca, caudal vertebra; caud, caudal surface; cav10–35, caudal vertebrae 10–35; cr, cervical rib; d, dentary; dr, dorsal ribs; dv, dorsal vertebrae; d1–d8, dorsal vertebrae 1–8; en, external naris; f, frontal; fc, contact for frontal; fe, femur; fib, fibula; il, ilium; is, ischium, j, jugal; la, lacrimal; lat, lateral surface; mt, metatarsal; mx, maxilla; na, nasal; naa, nasal arch; nc, neurocranium; pd, predentary; pf, prefrontal; plex, plexiform vascular arrangement; pm, premaxilla; pa, parietal; po, postorbital; pmc, contact for premaxilla; pu, pubis; qj, quadratojugal; qu, quadrate; rdp, rostrodorsal process; ret/long, reticular/longitudinal vascular arrangement; sa, surangular; sc, scapula; sq, squamosal; sr, sacral rib; tib, tibia.

2 | SYSTEMATIC PALEONTOLOGY

Dinosauria (Owen 1842).
Ornithischia (Seeley 1888).
Ornithopoda (Marsh 1881).
Iguanodontia (Dollo 1888 sensu Sereno 1998).
Hadrosauridae (Cope 1870 sensu Sereno 1998).
Hadrosaurinae (Lambe 1918 sensu Sereno 1998).
Kritosaurini (Brett-Surman 1989 sensu Prieto-Márquez, 2014b).
Gryposaurus (Lambe 1914).
Gryposaurus notabilis (Lambe 1914).

2.1 | Holotype

CMN 2278, a nearly complete articulated skull and postcranium (the latter partly unprepared), including skin impressions.

2.2 | Referred specimens

AMNH 5350, articulated partial cranium with associated right dentary, incomplete postcranium; CMN 2815, skull roof; CMN 8784, nearly complete skull, most of postcranium; CMN 12440, skull roof; CMN 57078, skull roof and partial braincase; MSNM V345, nearly complete skeleton missing caudal dorsals, most of sacrum, and ilia; ROM 764 (holotype of *Gryposaurus* "*incurvimanus*"), skull missing rostrum, nearly complete articulated skeleton lacking distal tail; ROM 873, partial articulated skull missing most of left circumorbital and infratemporal regions; ROM 1939, nearly complete left nasal and paired dentaries; TMP 1980.022.0001, incomplete, articulated skull missing right half of rostrum, partial postcranium; TMP 1991.081.0001, nearly complete, partially articulated skull missing quadrates and postdentary bones.

2.3 | Occurrence

Lower Dinosaur Park Formation (upper Campanian), Dinosaur Provincial Park and southern Alberta, Canada.

2.4 | Revised diagnosis

Large kritosaurin hadrosaurine characterized by the following unique combination of features, most readily visible in osteologically mature individuals: subtriangular denticles of the premaxilla and predentary slightly wider than tall (shared with *Bactrosaurus johnsoni*, *Gryposaurus latidens*, and *Gryposaurus monumentensis*, ? *Gryposaurus alsatei*); dorsolateral flaring on the medial margin of the caudoventral process of the premaxilla (autapomorphy of *Gryposaurus*, shared with *G. latidens* and *G. monumentensis*); dorsally convex nasal arch that extends well above the level of the frontals, the apex of which occurs between the external naris and orbit (shared with *Aralosaurus tuberiferus*, *G. latidens*, and *G. monumentensis*); U-shaped caudal margin of the external naris entirely formed by the nasal, and ventrally limited by a thick rostroventral flange of the bone (shared with Brachylophosaurini); caudodorsal margin of the circumnarial depression gently incised and located dorsal to the rostral half of the lacrimal (autapomorphy of *Gryposaurus*, shared with *G. latidens* and *G. monumentensis*); sigmoidal nasofrontal suture characterized by a small median process of the conjoined nasals inserting between the midline of the frontals (autapomorphy of *Gryposaurus*, shared with *G. latidens* and *G. monumentensis*); elevation of the caudal temporal region above the level of the frontals, reflected in the strongly caudodorsally canted intertemporal bar of the postorbital (shared with *Rhinorex condrupus*, *G. latidens*, and *G. monumentensis*); infratemporal fenestra rostrocaudally wider and dorsoventrally deeper than the orbit (shared with *Kritosaurus navajovius* and *R. condrupus*); subcircular mandibular "foramen" (sensu Gates & Sampson, 2007) (shared with some *Prosaurolophus maximus* and *B. canadensis*); massive proximodorsal corner of the paroccipital process with a thickness that is greater than the maximum mediolateral width of the foramen magnum (autapomorphy of *Gryposaurus*, shared with *G. latidens* and *G. monumentensis*).

2.5 | Remarks

The most recent diagnoses of *Gryposaurus notabilis* are those of Gates and Sampson (2007) and Prieto-Márquez (2010). However, some of the autapomorphies proposed by those authors are not limited to the species. We therefore offer a revised diagnosis here that we believe better reflects the attributes of *G. notablis*.

3 | DESCRIPTION OF CMN 8784

3.1 | Provenance

CMN 8784 was discovered in 1913 by W. E. Cutler and collected by B. Brown in what is now Dinosaur Provincial Park, Alberta. It was preserved within a channel sandstone in the lower Dinosaur Park Formation,

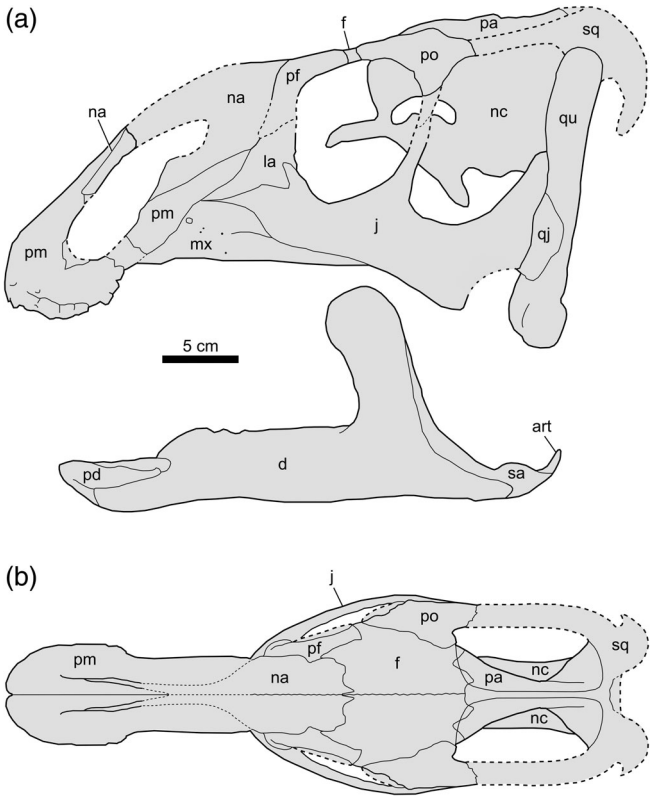

FIGURE 1 Skull reconstruction a *Gryposaurus notabilis*, based on CMN 8784 (with missing details of the nasal arch from ROM 1939). (a) Left lateral view; (b) dorsal view.

approximately 7.5 m above the lower formational contact (Lowi-Merri & Evans, 2020).

3.2 | Skull

The skull of CMN 8784, which is badly crushed, was adequately described and figured by Waldman (1969); however, we produced the first schematic reconstruction of the skull for this study. We therefore focus here on those gross morphological differences between our reconstruction of the skull and larger *Gryposaurus notabilis* skulls.

In overall proportions, the skull of CMN 8784 (Figure 1) resembles that of many non-hadrosaurid hadrosauroids (e.g., *Eolambia caroljonesa*, *Gobihadros mongoliensis*, *Tethyshadros insularis*) rather than adult hadrosaurids: the skull is relatively short, caudally narrow, and essentially unadorned, and the orbit is large. In these respects, the ontogenetic trends in the gross skull proportions of *G. notabilis* recall those seen in other hadrosaurids, including the hadrosaurines *P. maximus* (Drysdale et al., 2018) and *S. angustirostris* (Bell, 2011), and the lambeosaurines *Hypacrosaurus* spp. (Evans, 2010; Brink et al., 2011), *Corythosaurus casuarius*, and *Lambeosaurus lambei* (Dodson, 1975; Evans, 2010). The rostral margin of the premaxilla of CMN 8784 is nearly vertical, but not as tall as that of large *G. notabilis* (e.g., CMN 2278, ROM 873, MSNM V345). The oral margin of the premaxilla has subtriangular denticles spaced far apart; the spacing of the denticles is relatively narrower in larger *G. notablis*. Although the nasal of CMN 8784 is mostly missing, that of the similar-sized ROM 1939 shows that the nasal arch was only weakly developed (see below) and rostrally positioned, most closely matching the condition seen in *G.* "*incurvimanus*" (Lowi-Merri & Evans, 2020). As noted by Waldman (1969), the asymmetrical rostral process of the jugal of CMN 8784 nearly separates the maxilla from the lacrimal laterally. These last two elements meet one another along a broad, horizontal contact in larger specimens. The dorsal extension of the jugal bordering the rostral rim of the orbit is much smaller in CMN 8784 than in much larger skulls. The caudal end of the skull is tall as in large *G. notabilis*, but the skull roof—though largely reconstructed—is not as strongly sloped in lateral profile (Farke & Herrero, 2014).

3.3 | Axial skeleton

The articulated postcranium (measurements in Table 1) is mostly complete (Figure 2) but not especially well preserved because the bone surface is badly eroded in many places. Waldman (1969) mentioned that, with the exception of some caudal vertebrae, the whole vertebral column is present. However, while it is true that a number of caudal vertebrae are missing, several cervical vertebrae are likewise not preserved. The few that are preserved, representing portions of the cranial and caudal cervical series, are in such poor condition as to not warrant detailed description. However, we figure the postcranium of the specimen and note its most salient anatomical features, as preserved.

At least seven cervical vertebrae can be counted. Three cranial cervicals are associated with the skull block, including the articulated atlas and axis (Waldman, 1969). The transition from the cervical to the dorsal series is difficult to establish because one grades gradually into the other. The dorsals are often distinguished by the presence of parapophyses on the neural arch (Horner et al., 2004); however, these details are obscured and/or poorly preserved on the specimen. Parks (1920) defined the first dorsal vertebra as that bearing an elongate rib (presumably, reaching the sternum). So defined, there appears to be 16 dorsals, in agreement with ROM 764 (Waldman, 1969). Associated ribs are not present beyond dorsal 12, but it is possible that the small, caudalmost dorsal ribs are not preserved. The neural spines of the first four dorsals (where preserved) are strongly inclined caudally (Figure 3). The neural spine

TABLE 1 Measurements from the skeleton of juvenile *Gryposaurus notabilis* (CMN 8784)

Element	Side	Variable	Measurement (mm)
Scapula	R	Max. height	>91 (incomplete)
Humerus	R	Min. shaft circumference	118
Femur	R	Max. length	516
		Max. diameter	67
		Min. diameter	55
Tibia	R	Length	>480 (incomplete)
Metatarsal II	R	Length	142
Metatarsal III	R	Length	185
Metatarsal IV	R	Length	134
Pedal phalanx II-1	R	Length	66
Pedal phalanx II-2	R	Length	17
Pedal phalanx II-3	R	Length	49
Pedal phalanx III-1	R	Length	63
Pedal phalanx III-2	R	Length	21
Pedal phalanx III-3	R	Length	17
Pedal phalanx III-4 (ungual)	R	broken	broken
Metatarsal II	L	Length	147
Metatarsal III	L	Length	197
Metatarsal IV	L	Length	166
Pedal phalanx II-1	L	Length	67
Pedal phalanx II-2	L	Length	18
Pedal phalanx III-1	L	Length	62
Pedal phalanx III-2	L	Length	51
Pedal phalanx IV-1	L	Length	51
Pedal phalanx IV-2	L	Length	10
Pedal phalanx IV-3	L	Length	11
Pedal phalanx IV-4	L	Length	13
Pedal phalanx IV-5	L	Length	41

Abbreviation: R, right L, left.

of dorsal 5 is broken near the base, but otherwise does not appear so inclined; a similar condition is present in ROM 764. The spines of the mid-dorsal series are not as elongate as in ROM 764. Waldman (1969:574) attributed this fact to "the presence of cartilage or weak ossification"; however, the vertebrae ossify soon after hatching in *Alligator mississippiensis* (Rieppel, 1993), and so it is more likely that the neural spines are simply broken here (as they are elsewhere along the column). Traces of the ossified tendon trellis can be seen as far forward as dorsal 6 (as in ROM 764).

The sacral vertebrae are exceedingly poorly preserved, particularly caudally. We echo Waldman's (1969) observation that the sacral ribs are incompletely fused to their vertebrae, evidenced by the fact that a single, unbroken rib is preserved lying atop its associated vertebra (Figure 4). The sacrum is too damaged to identify its vertebral count.

An articulated series of 29 relatively complete caudal vertebrae is preserved in a single block (Figure 5). Judging by the three additional, distally angled chevrons preserved at the proximal end of the series (which appear to be the proximal-most chevrons), and assuming the numbers correspond to those of ROM 764 (Parks 1920), the 32 vertebrae represent caudals 8–36.

In overall shape and angulation of the various neural spines, the caudals closely resemble those of ROM 764, which preserves fewer distal tail vertebrae. The angle and attenuation of the caudal neural spines are less consistent in the very large MSNM V345 (Bertozzo et al., 2017), such that the dorsal profile of the tail in that

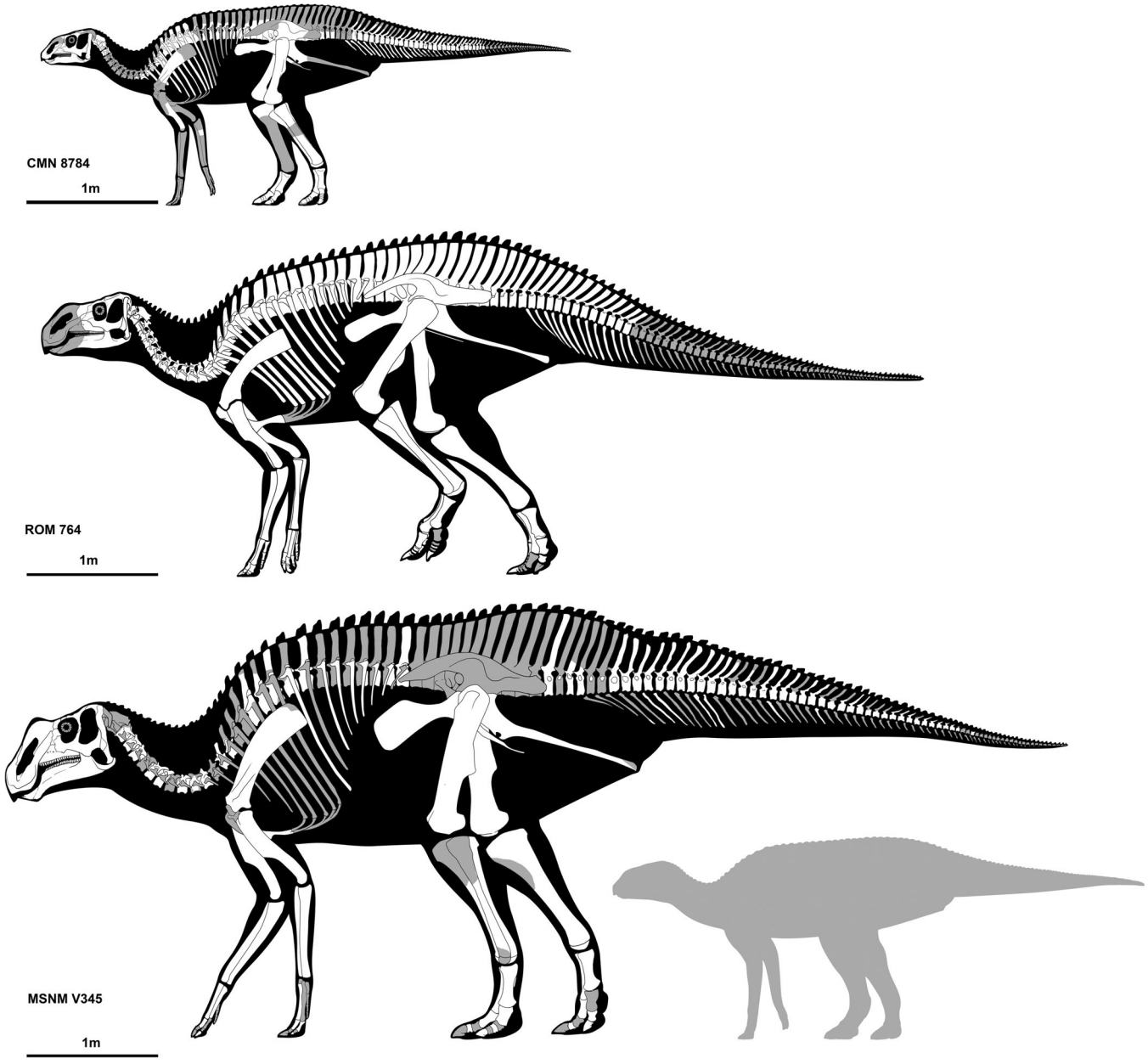

FIGURE 2 Skeletal reconstructions of a juvenile (CMN 8784), subadult (ROM 764), and adult (MSNM V345) *Gryposaurus notabilis*. Elements in gray are missing. Silhouette of CMN 8784 next to MSNM V345 emphasizes their size disparity.

specimen appears "wavy". Transverse processes of the vertebrae of CMN 8784 are little more than low swellings (likely eroded) and do not continue beyond caudal 17 (compared to caudal 21 in MSNM V345). The chevrons attenuate by caudal 20 (compared to caudal 44 in MSNM V345). The distalmost caudal vertebrae (which presumably lacked spinous processes altogether) are missing, although the total number of caudals probably did not approach the nearly 50 observed in MSNM V345 (Bertozzo et al., 2017). Toward the distal end of the tail, the caudal centra progressively reduce in height, similar to the condition in other hadrosaurids.

3.4 | Appendicular skeleton

Little is preserved of the pectoral girdle and forelimb. A portion of the right, strap-like scapular blade is preserved, overlying the ribcage (Figure 3). It is especially thin mediolaterally and bears two adjacent and longitudinally arrayed perforations of unknown origin (each ~40 mm long). The deltoid ridge is not preserved. A portion of the right humerus is preserved, missing the expanded proximal half, including the entirety of the deltopectoral crest (Figure 6). The distal condyles are about as well-developed as in both ROM 764 and MSNM V345.

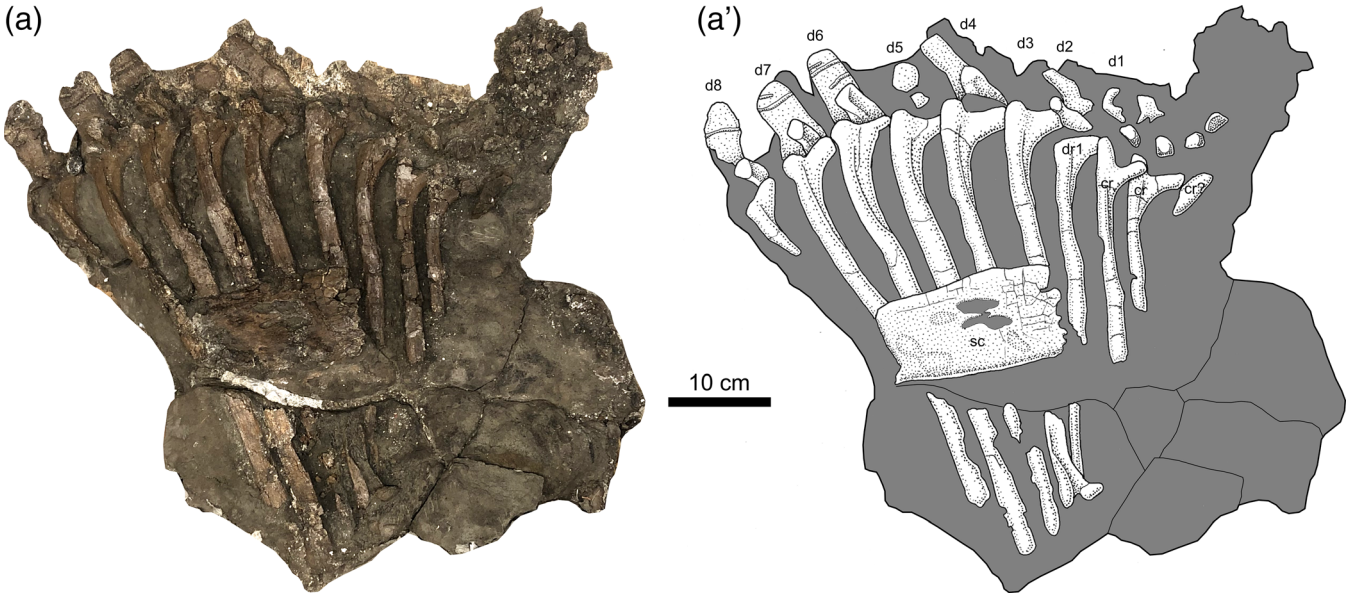

FIGURE 3 Right thoracic region of a juvenile *Gryposaurus notabilis* (CMN 8784). (a) Photograph; (a') interpretive drawing (gray indicates matrix).

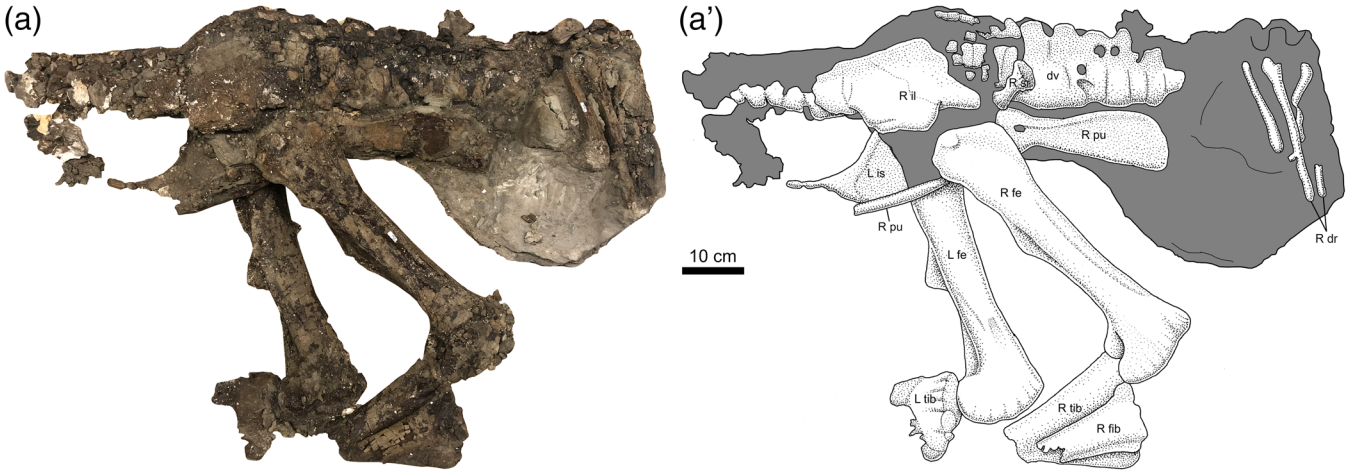

FIGURE 4 Right pelvic region of a juvenile *Gryposaurus notabilis* (CMN 8784). (a) Photograph; (a') interpretive drawing (gray indicates matrix).

Waldman (1969) described the pelvis as slender overall; however, much of the exposed ilium and ischium are missing, so that their precise shapes are difficult to confidently characterize. The supraacetabular process (= antitrochanter) of the ilium is as well-developed and lateroventrally pendant as in ROM 764, and shows a roughly U-shaped lateral outline, as in large *Gryposaurus notabilis* (e.g., ROM 764) and *Gryposaurus latidens* (AMNH 5465) (Prieto-Márquez, 2012). The apex of the supraacetabular process is situated immediately caudodorsal to the acetabulum (Figure 4). The prepubic process of the pubis is subequal in length to the rod-like postpubic process. The former is mediolaterally flattened, with a subrectangular cranial blade that is more expanded ventrally than dorsally. The cranial blade of the prepubic process is less cranioventrally inclined and proportionally narrower dorsoventrally (compared with the proximal neck) than that of large *Gryposaurus* spp. (e.g., AMNH 5465 and MSNM V345). The process strongly projects cranially such that it runs subparallel to the ventral margin of the dorsal vertebral column. By contrast, the prepubic process is angled cranioventrally in the articulated skeleton of ROM 764. We concur with Waldman's (1969) observation that there is an unusual small foramen that pierces the base of the prepubic process (Figure 4), but have no better insight as to its origin.

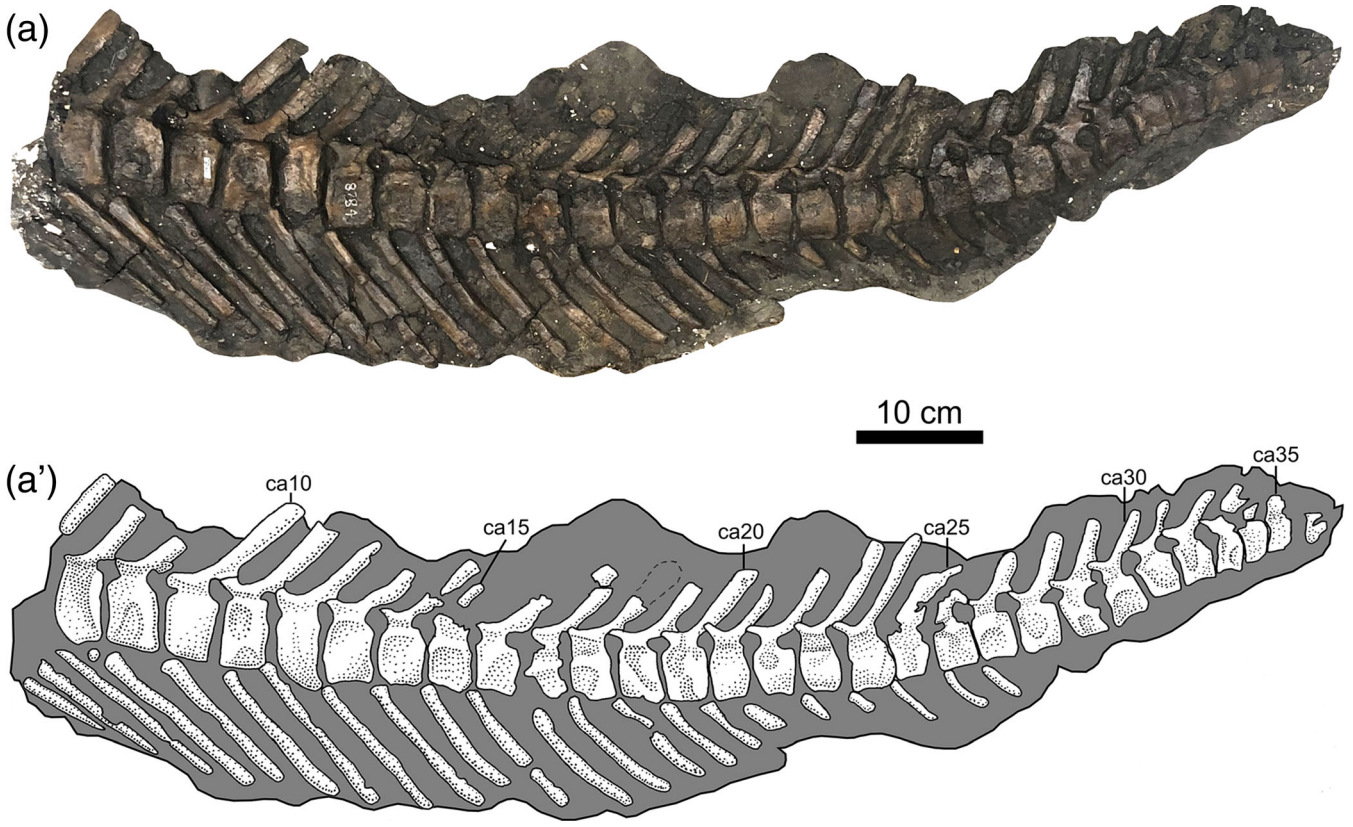

FIGURE 5 Caudal vertebrae of a juvenile *Gryposaurus notabilis* (CMN 8784) in left lateral view. (a) Photograph; (a') interpretive drawing (gray indicates matrix).

The femora are robust and bear all the various trochanters and condyles seen in adult specimens. The fourth trochanter, situated mid-way down the length of the shaft, varies between the right and left sides. On the left side, the trochanter is narrow-based, and the triangular apex is well-defined. On the right side, the trochanter is broad-based and low (Figure 4). The two distal condyles are well-developed and caudally expanded, as in larger individuals. The wing-like cnemial crest of the tibia is large and curves craniolaterally, as in larger specimens. The tibiae and fibulae are each broken at their proximal ends and cannot be reconnected with their distal ends, because the mid-shafts are missing. By combining the lengths of the preserved proximal and distal portions on the better-preserved right side, it is possible to estimate that the zeugopodium was at least 93% the length of the femur, and possibly somewhat longer. Of the tarsal elements, only the right astragalus is visible (Figure 7); the adjacent calcaneum is hidden by the overlying metatarsals of the right foot. The astragalus appears fully formed and articulates with the zeugopodium. Although incomplete, the right pes agrees in most respects with the proportions of ROM 764; however, the only preserved ungual of digit I is more strongly spade-shaped with broader "shoulders" compared to its homologue in ROM 764.

4 | DESCRIPTION OF ROM 1939

4.1 | Provenance

ROM 1939 was collected in modern-day Dinosaur Provincial Park, approximately 9 m above the base of the Dinosaur Park Formation.

4.2 | Skull

The left nasal is virtually complete, except for the rostral terminus of the dorsal premaxillary process (Figure 8). The nasal arch is weakly developed with an apex situated slightly rostral to the caudal margin of the external naris. The rami forming each side of the arch create an angle of approximately 140°, which is more obtuse than in other known specimens. The specimen more nearly approximates the low nasal arch of TMP 1980.022.0001 (= 132°, traditionally referred to *G. "incurvimanus"*), and contrasts with the condition seen in AMNH 5350 (= 113°),

FIGURE 6 Partial right humerus of *Gryposaurus notabilis* (CMN 8784). (a) Caudal view; (b) cranial view.

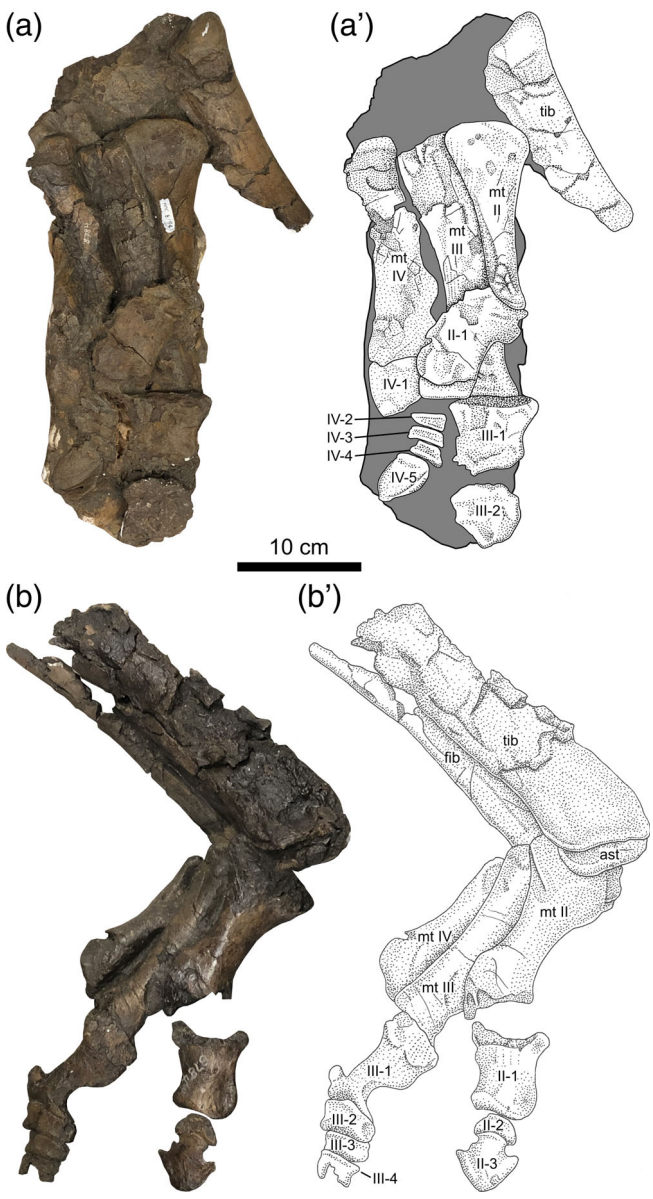

FIGURE 7 Distal hindlimbs of juvenile *Gryposaurus notabilis* (CMN 8784). Left distal hindlimb in ventral view: (a) photograph; (b) interpretive drawing (gray indicates matrix). Right distal hindlimb in dorsomedial view: (c) photograph; (d) interpretive drawing.

CMN 2278 (= 107°), and ROM 873 (= 105°). The caudal margin of the external naris forms a tightly circumscribed U-shape, more like that seen of ROM 873, CMN 2278, and AMNH 5350, but unlike specimens historically assigned to *G. "incurvimanus"* (i.e., ROM 764, TMP 1980.022.0001) in which the caudal end of the naris has a broad U-shape (Horner et al., 2004; Gates & Sampson, 2007). On the caudoventral surface of the bone, a series of longitudinal ridges marks the contact surface for the frontal, indicating that the caudal end of the bone is complete such that the distance of the nasal arch from the frontal contact can be reliably measured. Just ventral to the caudal margin of the external naris, the hook-like rostroventral flange of the nasal is dorsoventrally deep and flares slightly laterally, as in large *G. notabilis*.

The paired dentaries are nearly complete, except that the left is missing the coronoid process, and the right is missing the rostral articulation for the predentary (Figure 9). They are short and stout compared to their homologues in more mature individuals, and retain a nearly complete compliment of teeth. Each dentary bears ~25 or 26 tooth "families" (sensu Mallon & Anderson, 2014), with no more than four teeth per family, up to three of which may contribute to the occlusal surface (Waldman, 1969 estimated 22 tooth families in CMN 8784). The number of tooth families increases to 32, with as many as five teeth per family, in larger individuals (Lull & Wright, 1942).

The left dentary appears to preserve a complete tooth row (Figure 10d–f), with 25 tooth families in a dental battery that measures 149 mm in total length. The aspect ratio of the tooth crowns (height:length) varies along the tooth row between 2.07 and 2.23, with a complete crown aspect ratio of 2.15 in the middle of the tooth row (at tooth position 13). Distinct secondary ridges are

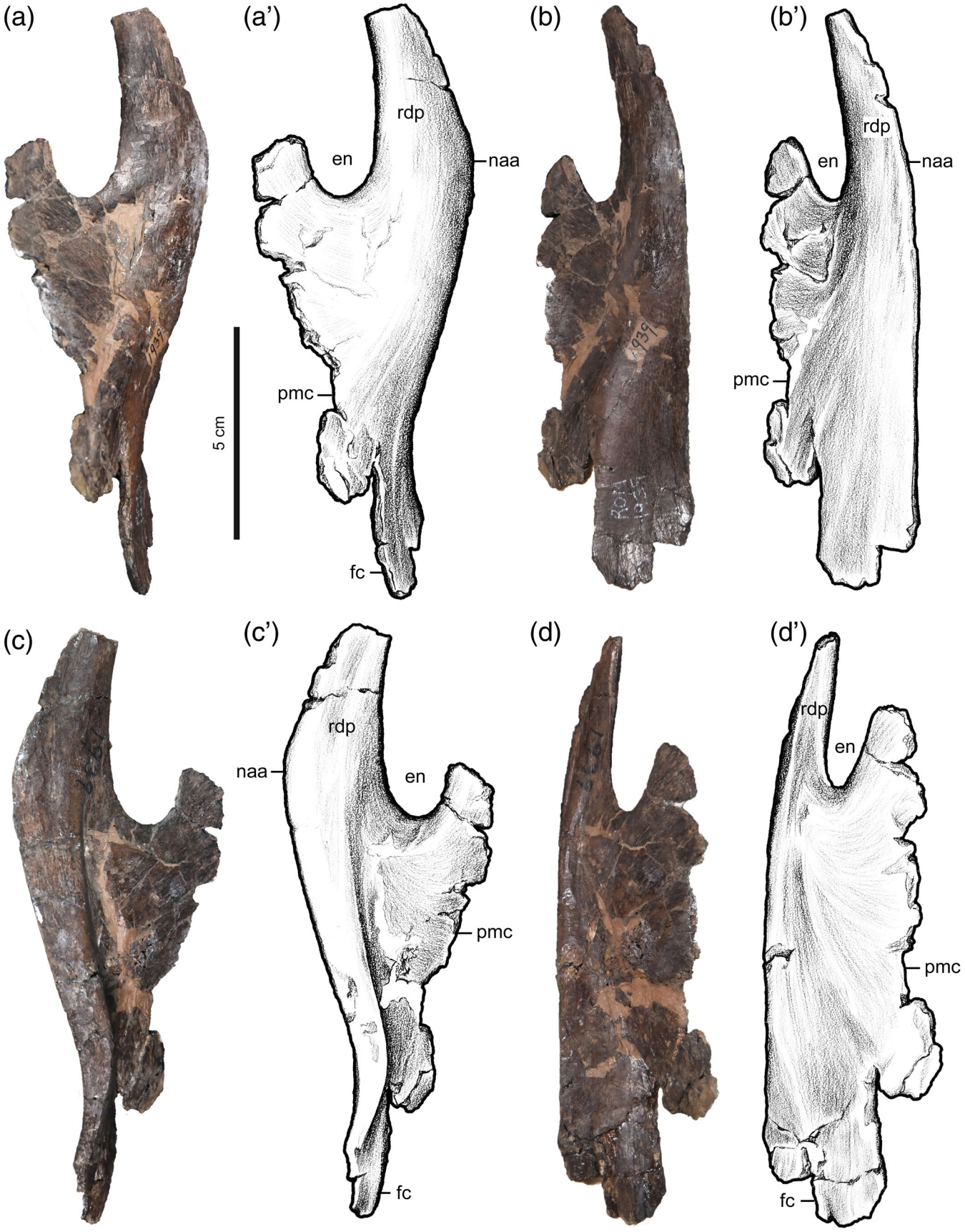

FIGURE 8 Left nasal of juvenile *Gryposaurus notabilis* (ROM 1939). Left nasal in: (a) lateral view; (a′) interpretive drawing of same; (b) dorsal view; (b′) interpretive drawing of same; (c) medial view; (c′) interpretive drawing of same; (d) ventral view; (d′) interpretive drawing of same.

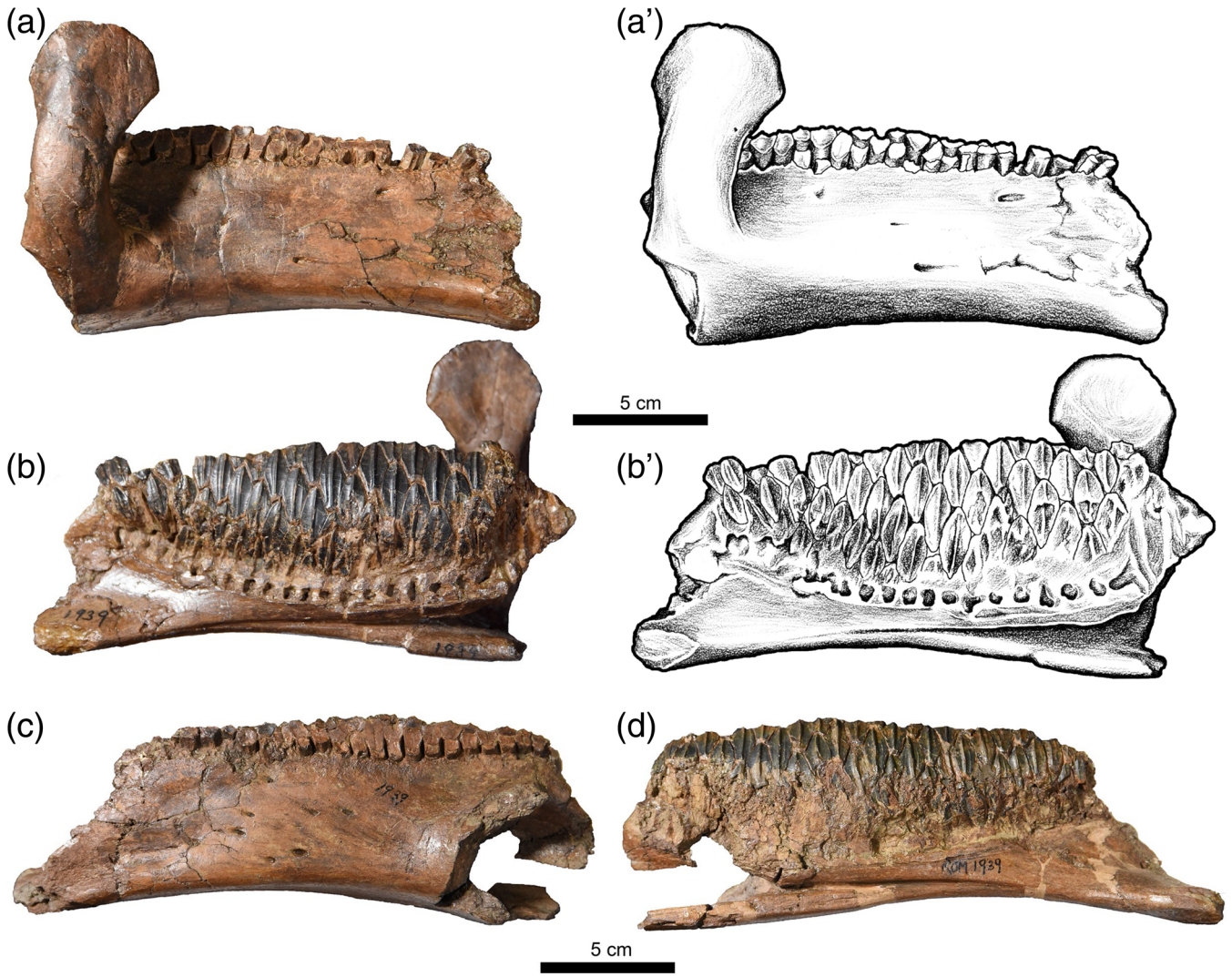

FIGURE 9 Dentaries of juvenile *Gryposaurus notabilis* (ROM 1939). Right dentary in lateral view: (a) photograph, (a') interpretive drawing; right dentary in medial view: (b) photograph, (b′) interpretive drawing; (c) left dentary in lateral view; (d) left dentary in medial view.

present on the mesial surface of the crown in almost all well-preserved crowns, where they typically span apicobasally from the top to the bottom of the crowns, and they are longest and most prominent in tooth families 8, 9, 10, 11, 12, 13, 18, 19, 20, and 22. Faint secondary ridges are also present on the distal half of the crown in tooth families 4, 6, 7, 9, 22, and 23, and they are most prominent in the apical part of the crown. Crowns in families 16, 17, 18, and 19 lack all secondary ridges on either side of the primary carina. Marginal papillae are not present on the dentition. Most tooth families contribute two teeth to the occlusal surface, but families 17 and 19 have three teeth forming the occlusal surface.

The right dentary has a complete coronoid process that is 41 mm long rostrocaudally (vs. 40 mm in CMN 8782) at its asymmetrically expanded apex. The dentition of the right dentary (Figure 10a–c) is not quite as complete as that of the left, but it passes caudally medial to the coronoid process, beyond its caudal margin. Although fewer teeth are preserved than in the left dentary, the tooth crowns at the center of the dental battery are complete with fine detail. The aspect ratio of a complete mid-dentary tooth crown (tooth family 13) is 2.29. Secondary ridges are present on the mesial half of the crown in families 2, 3, 4, 6, 7, 8, 10, 12, 13 and 20, and present distally in families 11, 17 and 18. Teeth in families 14, 15, and 16 lack any secondary ridges on either side of the carina and all teeth lack discernable marginal papillae.

Individually, the teeth contrast markedly with those of adult *G. notabilis*. Although the enameled tooth crowns retain a diamond shape, they are relatively wider (height/width = 2.07–2.29) than in adults (height/width = 2.5–2.7; Bertozzo et al., 2017). Each tooth is

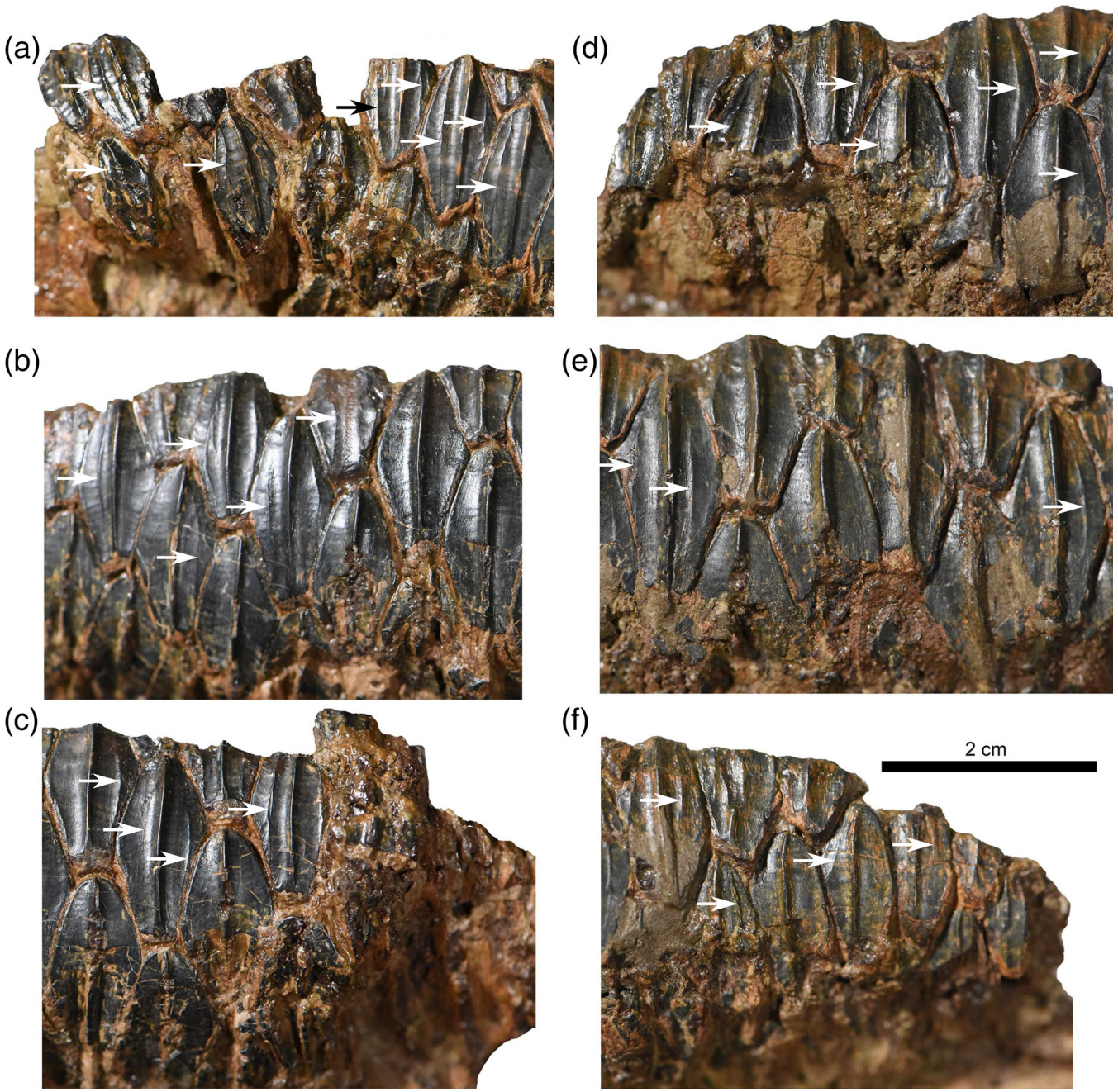

FIGURE 10 Dentary teeth of juvenile *Gryposaurus notabilis* (ROM 1939) in lingual view. (a)–(c) right tooth battery; (d)–(f) left tooth battery. (a) Mesial dentition; (b) middle dentition; (c) distal dentition. (d) distal dentition; (e) middle dentition; (f) mesial dentition. Arrows indicate secondary ridges.

bisected by a straight to slightly sinusoidal longitudinal (primary) ridge, which may or may not be associated with secondary ridges, either singly (fore or aft of the primary ridge) or paired. Neither the frequency nor the position of the secondary ridges appears to correspond with position within the tooth row. Notably, secondary ridges do not occur in more mature individuals of *G. notabilis* (Parks, 1920; Bertozzo et al., 2017). The smooth external margins of each tooth crown also contrasts with the finely papillated condition of the adults.

5 | OSTEOHISTOLOGICAL ANALYSIS OF CMN 8784

5.1 | Methods

A histological thin-section of the right ulna of CMN 8784 was made approximately 1/3 down length the shaft, to assess its ontogenetic age (other bones were unavailable for sampling). The section was made using standard techniques outlined in Lamm (2013) in the palaeohistology

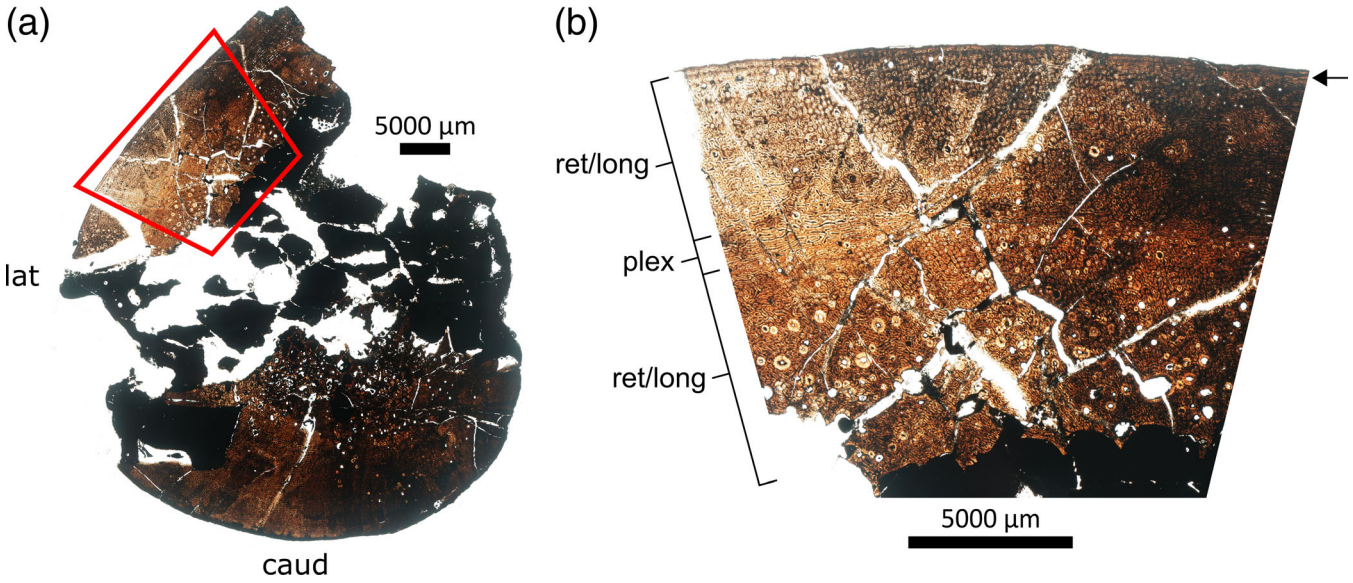

FIGURE 11 Histology of *Gryposaurus notabilis* juvenile (CMN 8784) showing transverse section of ulna. (a) Gross histological section. Trapezoid denotes detail shown in (b). (b) Detail of cortex in (a) showing zonal primary tissue and single Line of Arrested Growth near periosteum (arrow).

TABLE 2 Statistics for reduced major axis regressions of cranial elements

Regression	*n*	Slope	95% CI	R^2	Permuted *p*	Allometric trend
Quadrate height versus skull length	6	0.87	0.49–1.00	.97	**.007**	Isometric
Naris to nasal arch versus quadrate height	6	2.02	1.59–2.37	.98	**.007**	Positive*
Jugal length versus quadrate height	7	0.91	0.77–1.19	.95	**.002**	Isometric*
Frontal to base of nasal arch versus quadrate height	7	0.66	0.37–2.02	.42	.13	–
Height of jugal below orbit versus quadrate height	7	0.91	0.58–1.17	.94	**.001**	Isometric*
Height of jugal below infratemporal fenestra versus quadrate height	7	1.19	0.75–1.48	.88	**.005**	Isometric*
Skull width between postorbitals versus quadrate height	7	1.17	0.38–1.34	.92	**.001**	Isometric
Length along frontal midline suture versus quadrate height	6	0.16	−0.35–0.41	.28	.26	–
Dentary height versus quadrate height	7	1.20	0.65–1.60	.90	**.003**	Isometric

Notes: Statistical significance ($\alpha = .05$) indicated in **bold**. Permuted *p*-values are calculated using 9,999 replicates. Asterisk (*) indicates agreement with the results of Lowi-Merri and Evans (2020).

laboratory at the Royal Ontario Museum. While cutting the bone, a thin metal rod was encountered. This was removed prior to mounting and grinding. First, the region of the section was stabilized with a reversible resin (Technovit 5071, Kulzer Technique) and cut with a Buehler Isomet 1000 diamond wafer blade, prior to grinding using a Variable Speed Grinder Crystal Master Pro12. The specimen was then glued to a plexiglass slide using thin viscosity adhesive. After the stud was trimmed using the Buehler Isomet saw, it was ground to optimal thickness using a Hillquist 1010 grinding cup, with 600 grit carbide powder and 1 µm aluminum oxide powder applied afterwards to achieve final thickness and polish. The resultant thin-section was then imaged with a Nikon AZ-100 microscope under plain and polarized light.

5.2 | Results

The transverse section of the partial right ulna (Figure 11) shows that the medullar cavity is small, and that trabecular bone makes up approximately half the radial thickness of the bone. The region of the section was heavily stained and reconstructed in plaster,

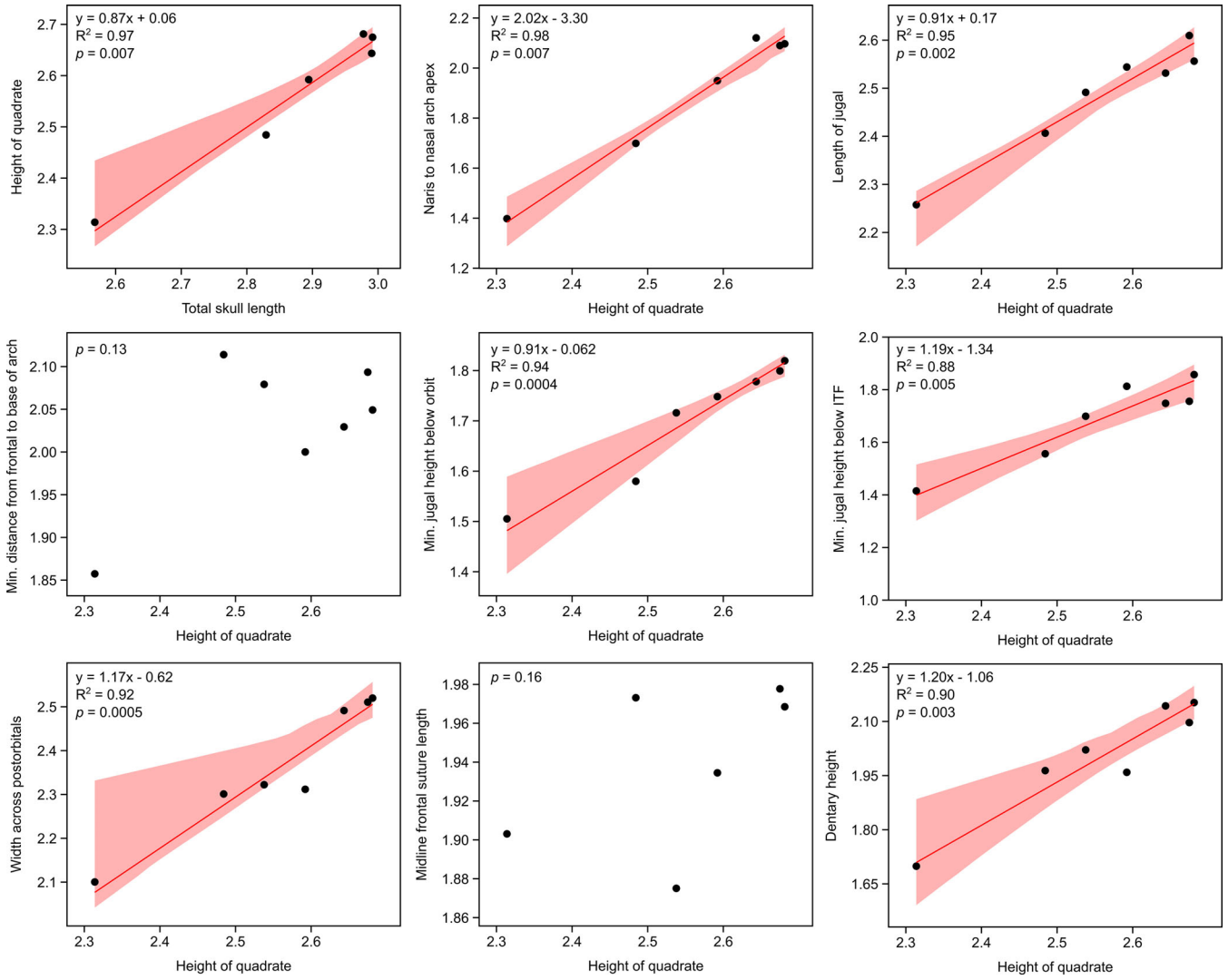

FIGURE 12 Reduced major axis regressions of skull elements in *Gryposaurus notabilis* (all measurements $\log_{10}$-transformed). In each plot, the red line represents the line of best-fit, and the concave hull indicates the 95% confidence interval. Plots without lines of best-fit show no significant correlation between variables.

limiting detailed histological observations. Where discernible, the primary tissue of the cortex consists of reticular fibrolamellar bone. Remodeling is reasonably widespread in the section, with secondary osteons most numerous in the inner cortex. The fibrolamellar primary tissue of the cortex is zonal, exhibiting the following pattern of vascular orientation types (from the inner cortex towards the periosteum): reticular/longitudinal (9.95 mm thick), plexiform (1.13 mm thick), reticular/longitudinal (4.58 mm thick). A single Line of Arrested Growth occurs immediately adjacent to the periosteum, but there is otherwise no sign of an external fundamental system. Similar early growth zones lacking LAGs have been described in the tibiae of similarly sized juvenile *Maiasaura peeblesorum* (Woodward et al., 2015), a closely related hadrosaurine, who noted the origin of this early cyclicity requires more research to determine if they represented annual growth marks. Nevertheless, the histology of the ulna supports a juvenile assignment for CMN 8784, an individual that was approximately 1–3 years of age based on comparisons with *M. peeblesorum* and *Edmontosaurus annectens* (Wosik & Evans, in press). Horner et al. (2000, 2009) showed that long bones of the hindlimb (i.e., femur, tibia) tend to retain a more complete record of cyclical growth in hadrosaurids, and so ours must be considered a minimum age estimate for CMN 8784.

6 | ALLOMETRIC ANALYSES

6.1 | Methods

Because CMN 8784 and ROM 1939 are so small compared to other available *Gryposaurus notabilis* material,

TABLE 3 Statistics for reduced major axis regression of postcranial elements

Regression	*n*	Slope	95% CI	R^2	*p* (two-tailed)	Allometric trend
Humerus shaft mediolateral diameter versus humerus length	6	0.90	0.63–1.49	.90	**.005**	Isometric
Humerus length versus femur length	6	1.69	−0.85–2.40	.68	**.032**	Isometric
Ulna length versus femur length	3	1.49	1.21–1.85	.99	.16	–
Maximum height of pubic blade versus minimum height of pubic blade	5	1.29	0.06–1.57	.95	**.009**	Isometric
Femur shaft rostrocaudal diameter versus femur length	5	0.96	−0.85–1.15	.90	**.007**	Isometric
Tibia length (CMN 8784 = 480 mm) versus femur length	7	0.94	0.27–1.00	.98	**.002**	Isometric
Metatarsal III length versus femur length	4	0.84	0.03–0.91	.99	**.043**	Negative

Notes: Statistical significance ($\alpha = .05$) indicated in **bold**. Permuted *p*-values are calculated using 9,999 replicates.

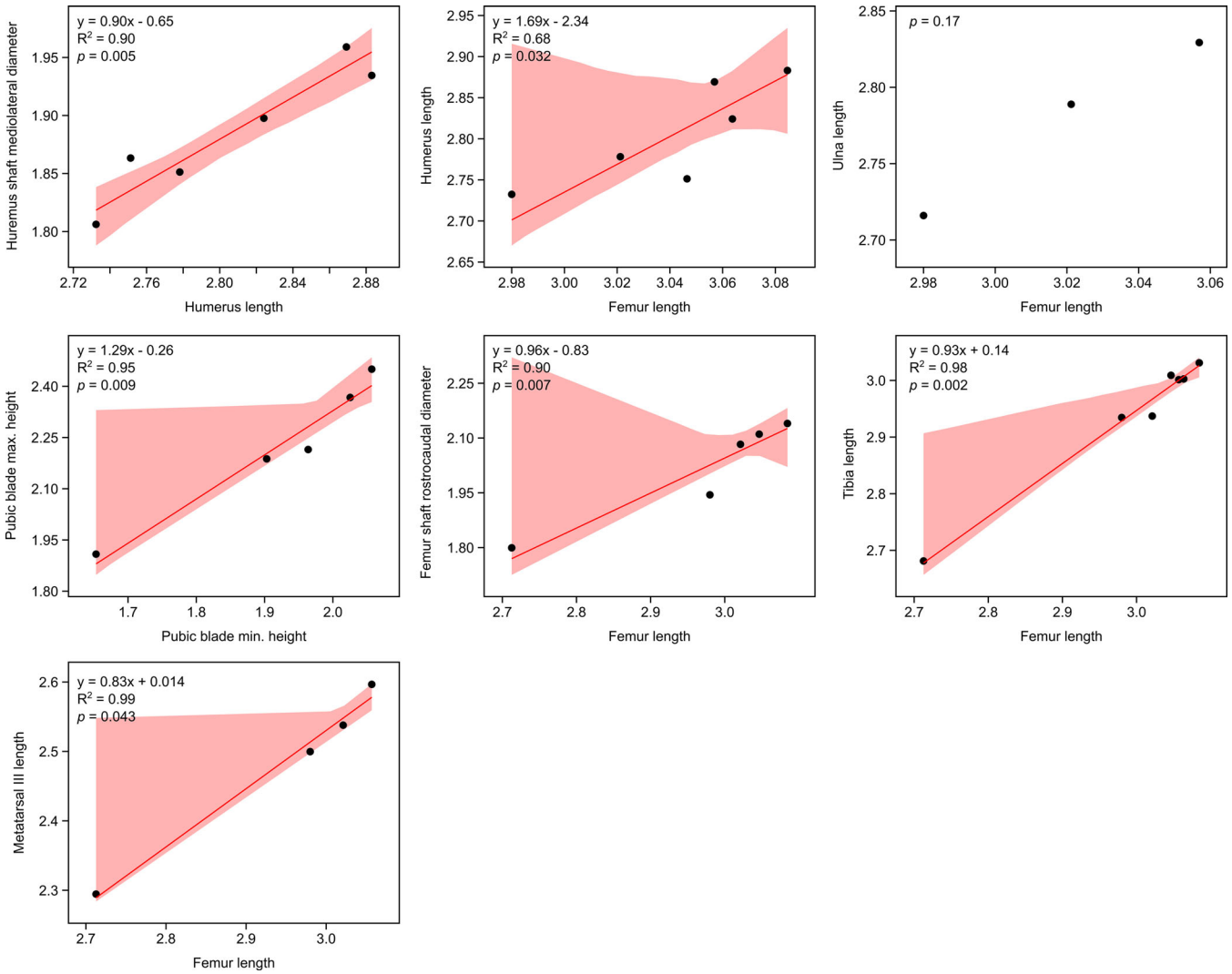

FIGURE 13 Reduced major axis regressions of postcranial elements in *Gryposaurus* (all measurements $\log_{10}$-transformed). In each plot, the red line represents the line of best-fit, and the concave hull indicates the 95% confidence interval.

TABLE 4 Allometric trends in the postcranium of select hadrosaurids

	Lambeosaurinae		Hadrosaurinae			
	Hypacrosaurus[a,b]	***Parasaurolophus***[c]	***Maiasaura***[a,b,d,e]	***Brachylophosaurus***[a]	***Edmontosaurus***[f–h]	***Gryposaurus***
Represented developmental stages	Nestling–adult	Juvenile–adult	Nestling–adult	Juvenile–adult	Nestling–adult	Juvenile–adult
Humerus length	?	Isometric	Negative	?	Isometric	Isometric
Humerus, minimum shaft diameter/circumference	?	?	Negative/positive	Isometric	Isometric	Isometric
Humerus, size of deltopectoral crest	Positive	?	Isometric/positive	Isometric	Isometric/positive	?
Humerus, development of distal condyles	?	?	Isometric	Positive	Positive	Isometric
Ulna, size of olecranon process	Isometric	?	Positive	Positive	Positive	?
Ilium, arching of preacetabular process	Positive	?	Positive	Positive	Positive	?
Ilium, projection of supra-acetabular crest	Positive	Positive	Positive	Positive	Positive	Positive
Pubis, height of blade	Positive	?	Isometric	Isometric	Isometric	Isometric
Femur, minimum diameter/circumference	Positive	?	Positive	?	Isometric/positive	Isometric
Femur, development of fourth trochanter	Positive	?	Positive	?	Isometric/positive	Positive
Femur, development of distal condyles	Positive	?	Isometric/positive	?	Positive	Isometric
Tibia, total length	?	Positive	?	?	Isometric	Isometric
Tibia, size of cnemial crest	Positive	?	Isometric/positive	?	Positive	?Isometric

Note: Trends for *Gryposaurus* not listed in Table 3 are inferred solely from visual comparison.

[a]Guenther (2009, 2014).

[b]Kilbourne and Makovicky (2010).

[c]Farke et al. (2013).

[d]Dilkes (2001).

[e]Prieto-Márquez and Guenther (2018).

[f]Prieto-Márquez (2014a).

[g]Wosik et al. (2017).

[h]Farke and Yip (2019).

they present a unique opportunity to test the cranial allometric trends recovered by Lowi-Merri and Evans (2020) by constraining the lower end of the growth curve. We therefore measured these specimens for seven of the ten linear variables used by Lowi-Merri and Evans (2020) (the remaining three variables were not preserved in either specimen). We also considered three new variables (width across postorbitals, midline frontal suture length, dentary height) to test related trends hypothesized by Waldman (1969).

Following Lowi-Merri and Evans (2020), we $\log_{10}$-transformed the data and subjected them to reduced major axis regression, implemented in PAST 4.06b (Hammer et al., 2001). Unless otherwise indicated, we used quadrate height as the independent variable because it scales isometrically with skull length in *G. notabilis* (see Results below) and other hadrosaurids and is more frequently preserved (e.g., Evans, 2010). We combined measurements from CMN 8784 and ROM 1939 to estimate the scaling relationships of nasal arch height relative to quadrate height because the specimens are nearly identical in size (where they overlap) and preserve complimentary material in this respect.

We also performed a preliminary allometric assessment of the postcranium of *Gryposaurus* using the methods above. Because sample sizes were small, we included the holotype of *Gryposaurus latidens* (AMNH 5465), assuming that allometric growth was similar across all members of the genus *Gryposaurus*, in the same way that they tend to be for species of the genus *Edmontosaurus* (Wosik et al., 2017). Unless otherwise indicated, we used femur length as our standard variable and proxy of size, which correlates strongly with body mass in vertebrates (Campione & Evans, 2012). We allowed the estimated length of the tibia to vary in order to understand how this might affect our allometric estimates. The raw data for all allometric analyses are available in Supplementary Data 1.

6.2 | Results

The cranial regression results are presented in Table 2 and Figure 12. Quadrate height scales isometrically with total skull length, supporting the initial assumption of Lowi-Merri and Evans (2020). Where our recovered allometric trends agree with those of Lowi-Merri and Evans (2020), our R^2 and *p*-values are generally higher, increasing the strength of these relationships. The only difference was in the relationship of the distance between the frontals and the base of the nasal arch versus quadrate height, which is insignificant here; Lowi-Merri and Evans (2020) noted that this allometric relationship was positive in their analyses (because the slope was >1), but their corresponding *p*-values were likewise insignificant. This is due to a relatively high degree of variation in this index, and highlights the need for larger sample sizes to understand growth patterns in this taxon.

Allometric trends in the postcranium are somewhat more ambiguous (Table 3; Figure 13), owing to smaller sample size and correspondingly wider confidence intervals. Where correlation is statistically significant, the proportions of the postcranium are not demonstrably allometric, except for metatarsal III length, which scales with negative allometry. The result for tibial scaling assumes a tibia 480 mm long for CMN 8784, which is simply the combined lengths of the preserved portions, which do not fit together cleanly. The reconstructed length must be inflated to 550 mm for this relationship to become significantly negatively allometric, which seems unlikely; this equates to 106% the length of the femur, which is quite inconsistent with what we observe in other hadrosaurids (*Parasaurolophus* sp., RAM 14000 = 93%; *E. annectens*, UCMP 128181 = 92%). An estimated tibia length closer to 480 mm therefore appears to be more realistic for CMN 8784.

7 | DISCUSSION

7.1 | Body size and overall growth rate

Waldman estimated that the total length of the skeleton of CMN 8784 was ~3.3 m; we estimate it closer to 4 m. Based on our reconstruction (Figure 2), the specimen is intermediate in overall length between LACM 23504 (juvenile *E. annectens*) at ~3.5 m and AMNH 5340 (juvenile *Lambeosaurus* sp.) at ~4.31 m. By comparison, the largest adult *Gryposaurus notabilis* measures up to 8.73 m long (Bertozzo et al., 2017). We estimated the body mass of CMN 8784 using stylopodial circumference scaling and developmental mass extrapolation (DME) implemented in the R package MASSTIMATE (Campione, 2020). Femur length was chosen as the scaling factor, using an adult body mass estimate of 4,312 kg (for AMNH 5350). In this way, we estimate the body mass of CMN 8784 to have been ~405 kg, or about the size of an average male Roosevelt elk (*Cervus canadensis roosevelti*).

The small body size and young osteohistological texture of CMN 8784 attest to its young age, probably between 1 and 3 years old. If we assume that CMN 8784 was two years of age, based on the interpretation of the first growth zone representing the first annulus, the animal had evidently reached almost 10% of its body mass in this time. This is somewhat less than the relative growth rate calculated for both *Maiasaura peeblesorum* and

E. annectens, which attained somewhere between 20% and 30% of their adult body masses within the same period of time (Woodward et al., 2015; Wosik et al., 2017). However, it is also possible that at least the first annual growth mark is completely missing due to bone remodeling, suggesting an even slower growth rate. Thus, *G. notabilis* appears to have grown more slowly at a rate more similar to that of *Probrachylophosaurus bergei* (Wosik et al., 2017). These comparisons are only preliminary, and further work on the osteochronology and growth dynamics of *G. notabilis* is required.

7.2 | Tooth ontogeny and taxonomy

Hadrosaurid tooth ontogeny is typically discussed in the context of the development of the dental battery (Erickson & Zelenitsky, 2014; Leblanc et al., 2016; Bramble et al., 2017); individual tooth development is not often considered. Among the few exceptions is *Hypacrosaurus stebingeri*, in which the teeth become relatively narrower with age, and increase the size and number of the marginal papillae (Horner & Currie, 1994). *Gryposaurus notabilis* is similar in these respects but differs in that—rather than developing secondary ridges with age, as in *H. stebingeri* (D. Zelenitsky pers. comm. to JCM, 2021)—the secondary ridges are lost. This is the first such documented instance of secondary ridge loss in hadrosaurid ontogeny, and evokes analogous discrete dental character changes in other dinosaurian taxa, such as the acquisition of serrations in tyrannosaurine premaxillary tooth ontogeny (Carr & Williamson, 2004; Currie, 2003), although this has recently been suggested to be more complex (Funston et al., 2021).

This new observation in *G. notabilis* dental ontogeny lends important perspective to the taxonomic debate viz. the edmontosaurin material from the Liscomb bonebed in Alaska (Gangloff & Fiorillo, 2010). This material was given the new name "*Ugrunaaluk kuukpikensis*" by Mori et al. (2016) but was soon deemed indistinguishable from *Edmontosaurus* spp. by Xing et al. (2017). Takasaki et al. (2020) later agreed that the Liscomb material is referrable to genus *Edmontosaurus* but resisted assigning the material to any of the known *Edmontosaurus* species (*E. regalis* and *E. annectens*; Campione & Evans, 2011) on account of some potentially diagnostic features. Among these, they listed secondary ridges of the teeth, which are not otherwise seen in those *Edmontosaurus* species known from Canada and the contiguous United States. The new information from *G. notabilis* documented here strongly suggests that the presence of secondary rides in young hadrosaurines is ontogenetically transitory and is not necessarily of any taxonomic significance. It suggests that at least some early-diverging hadrosaurines retained plesiomorphic dental characters early in ontogeny.

7.3 | Cranial allometry and implications

In most aspects considered here, the skull elements of *Gryposaurus notabilis* scale isometrically. This observation runs counter to some claims originally made by Waldman (1969) when describing the skull of CMN 8784. For example, he noted that the skull of this specimen was taller caudally relative to its length than in adult *G. notabilis*, implying that the caudal height of the skull scales with negative allometry. Our reconstruction (Figure 1) does not support his interpretation and, assuming for the moment that quadrate height approximates caudal skull height, nor does our allometric analysis. Interestingly, although the relationship we recovered between quadrate height and skull length is isometric (or possibly only weakly negatively allometric), Farke and Herrero (2014) found that caudal skull height in *Gryposaurus*, in fact, scales with positive allometry when gauged by the flexion of the postorbital in lateral view. Thus, if the quadrate does not scale concordantly, the difference must be made up for by a dorsoventral thickening of the squamosal, with which the quadrate articulates dorsally. This appears to be the case (see Farke & Herrero, 2014:Figure 11.1).

Waldman (1969) also noted that, perhaps surprisingly, the frontal length of CMN 8784 is nearly three-quarters that of the *G. notabilis* holotype (in fact, it is greater still; see Table 1). It is tempting to conclude that frontal length must therefore have scaled with negative allometry for the remainder of the animal's growth, but our data do not bear this out. Rather the rostrocaudal length of the frontal is highly variable, and there appears to be no strong relationship with quadrate height (Figure 12), which is almost certainly related to small sample size (Brown & Vavrek, 2015). The result nevertheless indicates that frontal length is among the most variable measures considered here ($R^2 = .28$). The highly variable length of the frontal that we document likely goes a long way toward explaining the variability we likewise recovered in the distance from the frontal to the base of the nasal arch. If the variation in frontal length is at least partially expressed at the rostral end of the element, then the distance to the nasal arch apex should vary accordingly. Our statistical results support this interpretation, as do those of Lowi-Merri and Evans (2020). Given the gross morphological differences in the placement of the nasal arch between small (e.g., ROM 1939) and large specimens (e.g., CMN 2278), we anticipate that further sampling will show that the minimum distance

from the frontal to the base of the nasal arch increases with negative allometry, consistent with the corresponding slope value given in Table 2.

Postorbital width did not scale as we had expected. Waldman (1969) observed that the skull of CMN 8784 is much narrower across the postorbitals compared to the holotype of *G. notabilis*, and implied that the caudal skull width of this species must have grown with positive allometry. We agree with Waldman's reasoning, but our statistical results do not bear this out; rather, skull width between the postorbitals scales isometrically relative to the quadrate length. This also may be a simple case of what Brown and Vavrek (2015) term "soft" isometry, where sample size is too small to return a significant allometric signal. However, the high R^2 value (.92) for this relationship implies otherwise. We offer instead that slight mediolateral crushing of some of the larger skulls (e.g., ROM 873, TMP 1991.081.0001, MSNM V345) may bias the signal.

Waldman (1969, p. 573) believed that the dentary of CMN 8784 was "fairly shallow", perhaps implying that the depth of the dentary grew with positive allometry. Our data do not support this either (Table 1). In fact, only the height of the nasal arch above the naris scales with positive allometry in our analysis (and that of Lowi-Merri & Evans, 2020). This result supports, but does not conclusively demonstrate, a role for sexual selection in the development of the arch (e.g., Knell et al., 2013). Importantly, the nasal arch is not entirely absent in either CMN 8784 or ROM 1939; rather, it is present but incipient. Other features characteristic of *G. notabilis* present in one or both of these specimens include the presence of subtriangular denticles of the premaxilla and predentary, a U-shaped caudal margin of the external naris bound entirely by the nasal, a sinusoidal nasofrontal suture, and an enlarged infratemporal fenestra. Thus, even juvenile individuals of *G. notabilis*, no more than a couple of years of age, might be identified from appropriate, isolated remains. This provides some reason to hope that the life history of *Gryposaurus* might be reconstructed even in the absence of abundant bonebed material, and yet such data are forthcoming (Scott et al., 2022).

Farke and Herrero (2014) reasoned that progressive flexion of the cranial vault of *G. notabilis* during ontogeny would have influenced the resulting bite mechanics by increasing the vertical component force exerted by the adductor musculature. This is true, but one might further ask what the effect was on overall applied bite force. Flexion of the cranial vault increases the length of the moment arm corresponding to the mandibular adductor musculature, which runs perpendicular between the force vector of those muscles and the jaw joint (Mallon & Anderson, 2015). However, this increase in the moment arm is only slight, and the effect on applied bite force was therefore probably negligible. Absolute bite force was probably much more greatly impacted by the overall increase in the size of the adductor musculature as the animal grew.

7.4 | Postcranial allometry and implications

The ontogenetic allometry of the hadrosaurid postcranium is becoming increasingly better understood (e.g., Egi & Weishampel, 2002; Brett-Surman et al., 2006; Baert et al., 2014; Wosik et al., 2017; Drysdale et al., 2018), including differences between the two subfamilies. Where determinable, ontogenetic scaling in the postcranium of *Gryposaurus* resembles that of other hadrosaurines in most respects (Table 4). *Gryposaurus* more closely resembles *Edmontosaurus* in that the development of the distal condyles of the femur scales isometrically, not with positive allometry as in *Hypacrosaurus stebingeri* and *M. peeblesorum*. The size of the cnemial crest of the tibia appears to scale isometrically in *Gryposaurus*, and with positive allometry in *M. peeblesorum*, *B. canadensis*, and *H. stebingeri*.

Wosik et al. (2017) demonstrated that, in *Edmontosaurus*, the fore- and hindlimbs scale essentially isometrically, both relative to one another and between elements within each limb (except for metatarsal III, which scales with weak negative allometry relative to the femur). They interpreted this to mean that the genus did not experience an ontogenetic gait shift, and that nestlings through adults habitually moved about quadrupedally. The details of limb scaling in *Gryposaurus* are consistent with the findings of Wosik et al. (2017). Not only do the limb elements appear to scale isometrically in *Gryposaurus* (except metatarsal III, which likewise scales with negative allometry relative to the femur), but the major limb muscle insertions (e.g., deltopectoral crest, fourth trochanter, cnemial crest) appear to scale with either isometry or positive allometry (Tables 3,4). This implies not only that there was not an associated gait shift in these taxa (cf. Wosik et al., 2017), but there were likewise little or no compensating musculoskeletal adaptations that would have allowed immature hadrosaurids to rival the locomotor performance of the more powerful adults (cf. Carrier, 1996; Herrel & Gibb, 2006). Such musculoskeletal adaptations are common, but not universal, among tetrapods, including in frogs (Emerson, 1978), lizards (Husak, 2006; Marsh, 1988), birds (Dial & Carrier, 2012), and mammals (Carrier, 1983; Young et al., 2010).

This inferred lack of performance compensation might come as some surprise, given evidence that at least some late juvenile to sub-adult hadrosaurids, between 1 and 4 years of age, lived apart from the protection of the adults (e.g., Paul, 1994; Varricchio, 2011; Wosik et al., 2020; Scott et al., 2022). These immature individuals were evidently highly subject to predation from large tyrannosaurids (Chin et al., 1998; Jacobsen, 1998; Varricchio, 2001), which might lead one to hypothesize that the selection pressure for compensatory locomotor performance was high (Carrier, 1996). The fact that this does not appear to have been the case suggests alternative behavioral adaptations (cf. Brecko et al., 2008; Irschick et al., 2000). Indeed, there is increasing evidence that juvenile hadrosaurids commonly formed small groups (Paul, 1994; Varricchio, 2011; Scott et al., 2022; Wosik & Evans, in press), which almost certainly provided some form of protection from predators. One might further speculate that these juvenile aggregations formed mutualistic associations with other herbivore groups, as seen in many plains-dwelling ungulates today (Sinclair, 1985), but this is going beyond the scope of the data.

All the above considerations must be tempered considering the nature of the evidence. The growth trends reconstructed for *Gryposaurus* spp. and *B. canadensis* in Table 4 are based on material spanning juvenile through adult growth forms; perinatal material is entirely unknown for these genera, and may yet influence the inferred allometries. Moreover, where nestling and early juvenile material is known for the remaining taxa, it tends to be susceptible to taphonomic damage, which may obscure or distort the original morphology (e.g., breakage of muscle crests). The same issue of "soft" isometry (discussed under "Cranial allometry and implications" above) is likely to apply, given the sparse data here.

8 | CONCLUSIONS

The rare juvenile material available for study extends the sampled ontogenetic sequence of *Gryposaurus notabilis*, which both provides new understanding of skeletal and dental ontogenetic development in the species and reinforces previously observed growth trends in the skull and postcranium. The loss of secondary ridges on the teeth with age, first documented here, provides crucial data for interpreting species richness based on immature hadrosaurid material (cf. Mori et al., 2016). The ontogeny of *G. notabilis* is among the better sampled for hadrosaurids, and yet it still is not as well sampled as *Maiasauria peeblesorum* or *Hypacrosaurus stebingeri*, for example. Even so, the available sample suggests that *Gryposaurus* were like other hadrosaurines in the development of the postcranium, most aspects of which grew isometrically or with positive allometry. These trends indicate that there likely was no strong selection for more efficient locomotor performance among young hadrosaurids. This hypothesis might be verified using the hadrosaurid trackway record (e.g., Currie et al., 1991; Fiorillo et al., 2014; Xing et al., 2009) to determine whether, for example, stride length similarly increases isometrically. If so, these hadrosaurids may have required compensating behavioral adaptations on their part to mitigate the predation pressures they faced, particularly from tyrannosaurids. The eventual discovery of still younger material, attributable to embryonic and perinatal individuals, will allow us to better constrain the allometric patterns documented here.

ACKNOWLEDGMENTS

First and foremost, our deep gratitude to our good friend and colleague, Peter Dodson, for his pioneering work on growth and allometry in the duck-billed dinosaurs and other reptiles. His contributions to the field continue to inspire and will long outlive us all. Thanks also to T. Lowi-Merri and T. Gates for sharing their photographs, to C. Brown for measurements of TMP 1980.022.0001, to M. Currie for collections help, to S. Rufolo for taking photographs, and to an anonymous artist for the skeletal drawings. Valuable discussion was provided by G. Gallimore, M. Guenther, A. Prieto-Márquez, M. Ryan, M. Wosik, and X.-C. Wu. Histological thin-sections of the ulna were provided by K. Chiba. The illustrations of ROM 1939 were executed by K. Dupuis, and the photographs of the specimen were taken by D. Dufault, who assisted with the figures. Funding to JCM and HX was provided by the National Natural Science Foundation of China (41602006), the Beijing Natural Science Foundation (5174032), the Beijing Millions of Talents Project in the New Century (2019A41), the State Key Laboratory of Palaeobiology and Stratigraphy of the Nanjing Institute of Geology and Paleontology (203120), the special financial support of the Beijing Government and the Canadian Museum of Nature. Funding to DCE was provided by Natural Sciences and Engineering Research Council Discovery Grant (NSERC Grant File Number: RGPIN-2018-06788). We are grateful to A. Fiorillo, C. Forster, and D. Weishampel for the invitation to contribute to this Festschrift.

ORCID

Jordan C. Mallon https://orcid.org/0000-0002-8209-8827
David C. Evans https://orcid.org/0000-0001-9608-6635
Hai Xing https://orcid.org/0000-0003-1198-4108

REFERENCES

Baert, M., Burns, M. E., & Currie, P. J. (2014). Quantitative diagenetic analyses of *Edmontosaurus regalis* (Dinosauria: Hadrosauridae) postcranial elements from the Danek Bonebed, Upper Cretaceous Horseshoe Canyon Formation, Edmonton, Alberta, Canada: Implications for allometric studies of fossil organisms. *Canadian Journal of Earth Sciences*, *51*, 1007–1016.

Bell, P. R. (2011). Cranial osteology and ontogeny of *Saurolophus angustirostris* from the Late Cretaceous of Mongolia with comments on *Saurolophus osborni* from Canada. *Acta Palaeontologica Polonica*, *56*, 703–722.

Bertozzo, F., Dal Sasso, C., Fabbri, M., Manucco, F., & Maganuco, S. (2017). *Redescription of a remarkably large Gryposaurus notabilis (Dinosauria: Hadrosauridae) from Alberta, Canada* (Vol. 43, pp. 1–56). Società Italiana di Scienze Naturali e Museo Civico di Storia Naturale.

Bramble, K., LeBlanc, A. R. H., Lamoureux, D. O., Wosik, M., & Currie, P. J. (2017). Histological evidence for a dynamic dental battery in hadrosaurid dinosaurs. *Scientific Reports*, *7*, 15787.

Brecko, J., Huyghe, K., Vanhooydonck, B., Herrel, A., Grbac, I., & Van Damme, R. (2008). Functional and ecological relevance of intraspecific variation in body size and shape in the lizard *Podarcis melisellensis* (Lacertidae). *Biological Journal of the Linnean Society*, *94*, 251–264.

Brett-Surman, M. K., Wagner, J. R., & Carpenter, K. (2006). Discussion of character analysis of the appendicular anatomy in Campanian and Maastrichtian North American hadrosaurids—Variation and ontogeny. In K. Carpenter (Ed.), *Horns and beaks: Ceratopsian and ornithopod dinosaurs* (pp. 135–169). Indiana University Press.

Brink, K. S., Zelenitsky, D. K., Evans, D. C., Therrien, F., & Horner, J. R. (2011). A sub-adult skull of *Hypacrosaurus stebingeri* (Ornithischia: Lambeosaurinae): Anatomy and comparison. *Historical Biology*, *23*, 63–72.

Brown, C. M., & Vavrek, M. J. (2015). Small sample sizes in the study of ontogenetic allometry; implications for palaeobiology. *PeerJ*, *3*, e818.

Campione, NE. 2020. MASSTIMATE: Body mass estimation equations for vertebrates. R package version 2.0-1. Placeholder Text-Placeholder Text https://CRAN.R-project.org/package=MASSTIMATE

Campione, N. E., & Evans, D. C. (2011). Cranial growth and variation in edmontosaurs (Dinosauria: Hadrosauridae): Implications for latest Cretaceous megaherbivore diversity in North America. *PLoS One*, *6*, e25186.

Campione, N. E., & Evans, D. C. (2012). A universal scaling relationship between body mass and proximal limb bone dimensions in quadrupedal terrestrial tetrapods. *BMC Biology*, *10*, 60.

Carr, T. D., & Williamson, T. E. (2004). Diversity of late Maastrichtian Tyrannosauridae (Dinosauria: Theropoda) from western North America. *Zoological Journal of the Linnean Society*, *142*, 479–523.

Carrier, D. R. (1983). Postnatal ontogeny of the musculo-skeletal system in the black-tailed jackrabbit (*Lepus californicus*). *Journal of Zoology*, *201*, 27–55.

Carrier, D. R. (1996). Ontogenetic limits on locomotor performance. *Physiological Zoology*, *69*, 467–488.

Chin, K., Tokaryk, T. T., Erickson, G. M., & Calk, L. C. (1998). A king-sized theropod coprolite. *Nature*, *393*, 680–682.

Currie, P. J. (2003). Cranial anatomy of tyrannosaurid dinosaurs from the Late Cretaceous of Alberta, Canada. *Acta Palaeontologica Polonica*, *48*, 191–226.

Currie, P. J., Nadon, G. C., & Lockley, M. G. (1991). Dinosaur footprints with skin impressions from the Cretaceous of Alberta and Colorado. *Canadian Journal of Earth Sciences*, *28*, 102–115.

Dewaele, L., Tsogtbaatar, K., Barsbold, R., Garcia, G., Stein, K., Escuillié, F., & Godefroit, P. (2015). Perinatal specimens of *Saurolophus angustirostris* (Dinosauria: Hadrosauridae), from the Upper Cretaceous of Mongolia. *PLoS One*, *10*, e0138806.

Dial, T. R., & Carrier, D. R. (2012). Precocial hindlimbs and altricial forelimbs: Partitioning ontogenetic strategies in mallards (*Anas platyrhynchos*). *Journal of Experimental Biology*, *215*, 3703–3710.

Dilkes, D. W. (2001). An ontogenetic perspective on locomotion in the Late Cretaceous dinosaur *Maiasaura peeblesorum* (Ornithischia: Hadrosauridae). *Canadian Journal of Earth Sciences*, *38*, 1205–1227.

Dodson, P. (1975). Taxonomic implications of relative growth in lambeosaurine hadrosaurs. *Systematic Biology*, *24*, 37–54.

Drysdale, E. T., Therrien, F., Zelenitsky, D. K., Weishampel, D. B., & Evans, D. C. (2018). Description of juvenile specimens of *Prosaurolophus maximus* (Hadrosauridae: Saurolophinae) from the Upper Cretaceous Bearpaw Formation of southern Alberta, Canada, reveals ontogenetic changes in crest morphology. *Journal of Vertebrate Paleontology*, *38*, e1547310.

Egi, N., & Weishampel, D. B. (2002). Morphometric analyses of humeral shapes in hadrosaurids (Ornithopoda, Dinosauria). *Senckenbergiana Lethaea*, *82*, 43–57.

Emerson, S. B. (1978). Allometry and jumping in frogs: Helping the twain to meet. *Evolution*, *32*, 551–564.

Erickson, G. M., & Zelenitsky, D. K. (2014). Osteohistology of *Hypacrosaurus stebingeri* teeth throughout ontogeny with comments on wear induced form and function. In D. A. Eberth & D. C. Evans (Eds.), *Hadrosaurs* (pp. 422–432). University of Indiana Press.

Evans, D. C. (2010). Cranial anatomy and systematics of *Hypacrosaurus altispinus*, and a comparative analysis of skull growth in lambeosaurine hadrosaurids (Dinosauria: Ornithischia). *Zoological Journal of the Linnean Society*, *159*, 398–434.

Farke, A. A., Chok, D. J., Herrero, A., Scolieri, B., & Werning, S. (2013). Ontogeny in the tube-crested dinosaur *Parasaurolophus* (Hadrosauridae) and heterochrony in hadrosaurids. *PeerJ*, *1*, e182.

Farke, A. A., & Herrero, L. (2014). Variation in the skull roof of the hadrosaur *Gryposaurus* illustrated by a new specimen from the Kaiparowits Formation (late Campanian) of southern Utah. In D. A. Eberth & D. C. Evans (Eds.), *Hadrosaurs* (pp. 191–199). Indiana University Press.

Farke, A. A., & Yip, E. (2019). A juvenile cf. *Edmontosaurus annectens* (Ornithischia, Hadrosauridae) femur documents a previously unreported intermediate growth stage for this taxon. *Vertebrate Anatomy Morphology Palaeontology*, *7*, 59–67.

Fiorillo, A. R., Hasiotis, S. T., & Kobayashi, Y. (2014). Herd structure in Late Cretaceous polar dinosaurs: A remarkable new dinosaur tracksite, Denali National Park, Alaska, USA. *Geology*, *42*, 719–722.

Funston, G. F., Powers, M. J., Whitebone, S. A., Brusatte, S. L., Scannella, J. B., Horner, J. R., & Currie, P. J. (2021). Baby tyrannosaurid bones and teeth from the Late Cretaceous of western North America. *Canadian Journal of Earth Sciences*, *58*, 756–777.

Gangloff, R. A., & Fiorillo, A. R. (2010). Taphonomy and paleoecology of a bonebed from the Prince Creek Formation, North Slope, Alaska. *PALAIOS*, *25*, 299–317.

Gates, T. A., & Sampson, S. D. (2007). A new species of *Gryposaurus* (Dinosauria: Hadrosauridae) from the late Campanian Kaiparowits Formation, southern Utah, USA. *Zoological Journal of the Linnean Society*, *151*, 351–376.

Guenther, M. F. (2009). Influence of sequence heterochrony on hadrosaurid dinosaur postcranial development. *Anatomical Record*, *292*, 1427–1441.

Guenther, M. F. (2014). Comparative ontogenies (appendicular skeleton) for three hadrosaurids and a basal iguanodontian: Divergent developmental pathways in Hadrosaurinae and Lambeosaurinae. In D. A. Eberth & D. C. Evans (Eds.), *Hadrosaurs* (pp. 398–415). Indiana University Press.

Hammer, Ø., Harper, D. A. T., & Ryan, P. D. (2001). PAST: Paleontological statistics software package for education and data analysis. *Palaeontologia Electronica*, *4*(1), 4.

Herrel, A., & Gibb, A. C. (2006). Ontogeny of performance in vertebrates. *Physiological and Biochemical Zoology*, *79*, 1–6.

Horner, J. R., & Currie, P. J. (1994). Embryonic and neonatal morphology and ontogeny of a new species of *Hypacrosaurus* (Ornithischia, Lambeosauridae) from Montana and Alberta. In K. Carpender, K. F. Hirsch, & J. R. Horner (Eds.), *Dinosaur eggs and babies* (pp. 312–336). Cambridge University Press.

Horner, J. R., De Ricqlès, A., & Padian, K. (2000). Long bone histology of the hadrosaurid dinosaur *Maiasaura peeblesorum*: Growth dynamics and physiology based on an ontogenetic series of skeletal elements. *Journal of Vertebrate Paleontology*, *20*(1), 115–129.

Horner, J. R., De Ricqles, A., Padian, K., & Scheetz, R. D. (2009). Comparative long bone histology and growth of the "hypsilophodontid" dinosaurs *Orodromeus makelai, Dryosaurus altus*, and *Tenontosaurus tillettii* (Ornithischia: Euornithopoda). *Journal of Vertebrate Paleontology*, *29*(3), 734–747.

Horner, J. R., Weishampel, D. B., & Forster, C. A. (2004). Hadrosauridae. In D. B. Weishampel, P. Dodson, & H. Osmólska (Eds.), *The Dinosauria* (2nd ed., pp. 438–463). University of California Press.

Husak, J. F. (2006). Does speed help you survive? A test with collared lizards of different ages. *Functional Ecology*, *20*, 174–179.

Irschick, D. J., Macrini, T. E., Koruba, S., & Forman, J. (2000). Ontogenetic differences in morphology, habitat use, behavior, and sprinting capacity in two west Indian *Anolis* lizards. *Journal of Herpetology*, *34*, 444–451.

Jacobsen, A. R. (1998). Feeding behaviour of carnivorous dinosaurs as determined by tooth marks on dinosaur bones. *Historical Biology*, *13*, 17–26.

Kilbourne, B. M., & Makovicky, P. J. (2010). Limb bone allometry during postnatal ontogeny in non-avian dinosaurs. *Journal of Anatomy*, *217*, 135–152.

Knell, R. J., Naish, D., Tomkins, J. L., & Hone, D. W. E. (2013). Sexual selection in prehistoric animals: Detection and implications. *Trends in Ecology & Evolution*, *28*, 38–47.

LeBlanc, A. R. H., Reisz, R. R., Evans, D. C., & Bailleul, A. M. (2016). Ontogeny reveals function and evolution of the hadrosaurid dinosaur dental battery. *BMC Evolutionary Biology*, *16*, 152.

Lowi-Merri, T. M., & Evans, D. C. (2020). Cranial variation in *Gryposaurus* and biostratigraphy of hadrosaurines (Ornithischia: Hadrosauridae) from the Dinosaur Park Formation of Alberta, Canada. *Canadian Journal of Earth Sciences*, *57*, 765–779.

Lull, R. S., & Wright, N. E. (1942). Hadrosaurian dinosaurs of North America. *Geological Society of America Special Papers*, *40*, 1–242.

Mallon, J. C. (2019). Competition structured a Late Cretaceous megaherbivorous dinosaur assemblage. *Scientific Reports*, *9*, 1–18.

Mallon, J. C., & Anderson, J. S. (2014). The functional and palaeoecological implications of tooth morphology and wear for the megaherbivorous dinosaurs from the Dinosaur Park Formation (upper Campanian) of Alberta, Canada. *PLoS ONE*, *9*, e98605.

Mallon, J. C., & Anderson, J. S. (2015). Jaw mechanics and evolutionary paleoecology of the megaherbivorous dinosaurs from the Dinosaur Park Formation (upper Campanian) of Alberta, Canada. *Journal of Vertebrate Paleontology*, *35*, e904323.

Marsh, R. L. (1988). Ontogenesis of contractile properties of skeletal muscle and sprint performance in the lizard *Dipsosaurus dorsalis*. *Journal of Experimental Biology*, *137*, 119–139.

Mori, H., Druckenmiller, P., & Erickson, G. (2016). A new Arctic hadrosaurid (Dinosauria: Hadrosauridae) from the Prince Creek Formation (lower Maastrichtian) of northern Alaska. *Acta Palaeontologica Polonica*, *61*, 15–32.

Parks, W. A. (1920). *The osteology of the trachodont dinosaur Kritosaurus incurvimanus* (Vol. 11, pp. 1–75). University of Toronto Studies, Geology Series.

Paul, G. S. (1994). Dinosaur reproduction in the fast lane: Implications for size, success, and extinction. In K. Carpenter, K. F. Hirsch, & J. R. Horner (Eds.), *Dinosaur eggs and babies* (pp. 244–255). Cambridge University Press.

Prieto-Márquez, A. (2010). The braincase and skull roof of *Gryposaurus notabilis* (Dinosauria, Hadrosauridae), with a taxonomic revision of the genus. *Journal of Vertebrate Paleontology*, *30*, 838–854.

Prieto-Márquez, A. (2012). The skull and appendicular skeleton of *Gryposaurus latidens*, a saurolophine hadrosaurid (Dinosauria: Ornithopoda) from the early Campanian (Cretaceous) of Montana, USA. *Canadian Journal of Earth Sciences*, *49*, 510–532.

Prieto-Márquez, A. (2014a). A juvenile *Edmontosaurus* from the late Maastrichtian (Cretaceous) of North America: Implications for ontogeny and phylogenetic inference in saurolophine dinosaurs. *Cretaceous Research*, *50*, 282–303.

Prieto-Márquez, A. (2014b). Skeletal morphology of *Kritosaurus navajovius* (Dinosauria: Hadrosauridae) from the Late Cretaceous of the North American south-west, with an evaluation of the phylogenetic systematics and biogeography of Kritosaurini. *Journal of Systematic Palaeontology*, *12*, 133–175.

Prieto-Márquez, A., & Guenther, M. F. (2018). Perinatal specimens of *Maiasaura* from the Upper Cretaceous of Montana (USA): Insights into the early ontogeny of saurolophine hadrosaurid dinosaurs. *PeerJ*, *6*, e4734.

Rieppel, O. (1993). Studies on skeleton formation in reptiles. V. Patterns of ossification in the skeleton of *Alligator mississippiensis* Daudin (Reptilia, Crocodylia). *Zoological Journal of the Linnean Society*, *109*, 301–325.

Ryan, M. J., & Evans, D. C. (2005). Ornithischian dinosaurs. In P. J. Currie, & E. B. Koppelhus (Eds.), *Dinosaur provincial park: A spectacular ancient ecosystem revealed* (pp. 312–348). Indiana University Press.

Scott, E. E., Chiba, K., Fanti, F., Saylor, B. Z., Evans, D. C., & Ryan, M. J. (2022). Taphonomy of a monodominant *Gryposaurus* sp. bonebed from the Oldman Formation (Campanian) of Alberta, Canada. *Canadian Journal of Earth Sciences*, *59*(6), 389–405.

Sinclair, A. R. E. (1985). Does interspecific competition or predation shape the African ungulate community? *Journal of Animal Ecology*, *54*, 899–918.

Takasaki, R., Fiorillo, A. R., Tykoski, R. S., & Kobayashi, Y. (2020). Re-examination of the cranial osteology of the Arctic Alaskan hadrosaurine with implications for its taxonomic status. *PLoS One*, *15*(5), e0232410.

Varricchio, D. J. (2001). Gut contents from a Cretaceous tyrannosaurid: Implications for theropod dinosaur digestive tracts. *Journal of Paleontology*, *75*, 401–406.

Varricchio, D. J. (2011). A distinct dinosaur life history? *Historical Biology*, *23*, 91–107.

Waldman, M. (1969). On an immature specimen of *Kritosaurus notabilis* (Lambe), (Ornithischia: Hadrosauridae) from the Upper Cretaceous of Alberta, Canada. *Canadian Journal of Earth Sciences*, *6*, 569–576.

Woodward, H. N., Freedman Fowler, E. A., Farlow, J. O., & Horner, J. R. (2015). *Maiasaura*, a model organism for extinct vertebrate population biology: A large sample statistical assessment of growth dynamics and survivorship. *Paleobiology*, *41*, 503–527.

Wosik, M., & Evans, D. C. (in press). Osteohistological and taphonomic life history assessment of *Edmontosaurus annectens* (Ornithischia: Hadrosauridae) from the Late Cretaceous (Maastrichtian) Ruth Mason dinosaur quarry, South Dakota, United States. *Journal of Anatomy*.

Wosik, M., Goodwin, M. B., & Evans, D. C. (2017). A nestling-sized skeleton of *Edmontosaurus* (Ornithischia, Hadrosauridae) from the Hell Creek Formation of northeastern Montana, USA, with an analysis of ontogenetic limb allometry. *Journal of Vertebrate Paleontology*, *37*, e1398168.

Wosik, M., Chiba, K., Therrien, F., & Evans, D. C. (2020). Testing size–frequency distributions as a method of ontogenetic aging: A life-history assessment of hadrosaurid dinosaurs from the Dinosaur Park Formation of Alberta, Canada, with implications for hadrosaurid paleoecology. *Paleobiology*, *46*(3), 379–404.

Wyenberg-Henzler, T., Patterson, R. T., & Mallon, J. C. (2022). Ontogenetic dietary shifts in north American hadrosaurids. *Cretaceous Research*, *135*, 105177.

Xing, H., Mallon, J. C., & Currie, M. L. (2017). Supplementary cranial description of the types of *Edmontosaurus regalis* (Ornithischia: Hadrosauridae), with comments on the phylogenetics and biogeography of Hadrosaurinae. *PLoS One*, *12*, e0175253.

Xing, L., Harris, J. D., Dong, Z., Lin, Y., Chen, W., Guo, S., & Ji, Q. (2009). Ornithopod (Dinosauria: Ornithischia) tracks from the Upper Cretaceous Zhutian Formation in the Nanxiong Basin, Guangdong, China and general observations on large Chinese ornithopod footprints. *Geological Bulletin of China*, *28*, 829–843.

Young, J. W., Fernández, D., & Fleagle, J. G. (2010). Ontogeny of long bone geometry in capuchin monkeys (*Cebus albifrons* and *Cebus apella*): Implications for locomotor development and life history. *Biology Letters*, *6*, 197–200.

SUPPORTING INFORMATION

Additional supporting information can be found online in the Supporting Information section at the end of this article.

How to cite this article: Mallon, J. C., Evans, D. C., Zhang, Y., & Xing, H. (2022). Rare juvenile material constrains estimation of skeletal allometry in *Gryposaurus notabilis* (Dinosauria: Hadrosauridae). *The Anatomical Record*, 1–23. https://doi.org/10.1002/ar.25021